Universitetet i Stavanger

FACULTY OF SCIENCE AND TECHNOLOGY

MASTER'S THESIS

Study program/specialization: Petroleum engineering Drilling and well engineering	Spring semester 2021 Open access
Author: Pouya Khalili	_____ (Author's signature)

Faculty Supervisor:
Arild Saasen
Mahmoud Khalifeh

Title of master's thesis:
Measuring the Magnetic Content of Drilling Fluid

Credits: 30 ECTS

Keywords: Drilling fluid contamination Magnetic particles Azimuth measurement Magnetic shielding Ditch magnet	Number of pages: X+ 64 Stavanger, 15th June 2021

Measuring the Magnetic Content of Drilling Fluid

By

Pouya Khalili

Master's Thesis

Presented to the Faculty of Science and Technology

University of Stavanger

University of Stavanger

June 2021

Acknowledgement

I would like to express my special thanks to my supervisors, Prof. Arild Saasen and Associate Prof. Mahmoud Khalifeh, who gave me this valuable opportunity and provided me with their continued support and encouragement. Secondly, I would like to thank Bodil Aase from Equinor ASA and Mona Wetrhus Minde from UiS for their productive advice and guidance. Also, I would like to thank Jagtech AS and Equinor ASA for supporting the project and providing the data. Finally, I am extremely grateful to my family for always being there and supporting me.

Abstract

Magnetic contamination of drilling fluid can impact the accuracy of the directional surveying by shielding the magnetic field. Additionally, this contamination, such as swarf or finer magnetic particles, can agglomerate on the downhole tool or BOP and cause tool failure in the worst-case scenario. Thus, making the measurement of the magnetic content of the drilling fluid necessary. However, there is no recommended practice in API or ISO for this purpose. A simple experimental setup and measurement system was developed that can be easily deployed in the rig site to measure the magnetic contamination of drilling fluid.

47 drilling fluid samples were collected from a multilateral production well drilled with a semi-submersible drilling rig located in one of the North sea's fields. The magnetic content of these samples was measured using the established method, and the microstructure of the collected content was analyzed using a Scanning electron microscope (SEM) and X-Ray Diffraction Analysis (XRD).

Ditch magnets are commonly installed in the flowline on the rig to remove the swarf and finer magnetic particles if their design is optimized. Ditch magnet measurement data of the well that the drilling fluid samples were collected from is presented. Operational details and common factors that might build up the production of the magnetic content were also investigated. By comparing the measured magnetic contamination of the drilling fluid samples and ditch magnet measurement data, it was possible to evaluate the efficiency of the ditch magnet system.

Acronyms

ISCWSA	Industry Steering Committee for Wellbore Survey Accuracy
IFR	Infield Referencing
IIFR	Interpolated Infield Referencing (IIFR)
EDS	Energy Dispersive X-Ray Spectroscopy
MSA	Multistation Analysis
NMR	Nuclear Magnetic Resonance
OBDF	Oil-Based Drilling Fluid
SEM	Scanning Electron Microscope
SI	International System of Units
XRD	X-Ray Diffraction
WBDF	Water-Based Drilling Fluid

List of Contents

List of Figures

List of Tables

1 Introduction

To hit the planned position of the last casing above the reservoir is very important to obtain proper drainage of the reservoir and to avoid well collision. The azimuth of the well, which is the orientation angle with respect to the north, is among those important parameters that help avoid costly mistakes if measured with high accuracy. Azimuth measurement is done using gyroscope and magnetometers. The former employs the earth's spin vector and the latter earth's magnetic field. Both these tools have some drawbacks; the gyros are not affordable and lose their accuracy when used in the Arctic region, and the magnetic compass suffers from magnetic interference. The best practice is to use them in a supportive manner where the gyro is used in the shallower section where near-wellbore magnetic interference is high, and the magnetometer is used in the deeper section.

One of the sources that can distort the earth's magnetic field measured by a downhole magnetic sensor is drilling fluid. Magnetic contamination in the drilling fluid can be from intentional origins such as weight material or unwanted origins such as metallic swarf, clay minerals, and other finer particles (Wilson and Brooks 2001). A Case study conducted by Saasen et al. showed that after cleaning the magnetic debris of drilling fluid, the accuracy of the wellbore survey increased to an acceptable level (Saasen et al. 2020). Although drill string interference is well-known in the industry, the magnetic content of drilling fluid is not among the source of errors in the error model that is introduced by The Industry Steering Committee for Wellbore Survey Accuracy (ISCWSA). Thus, cleaning the magnetic content of the drilling fluid effectively remains the only option to improve the quality of the survey. To do that, ditch magnets are stationed in the flowline before or after shale shaker on the offshore rigs.

Several experimental works investigated the effect of different drilling fluid additives in shielding the magnetic field (Amundsen et al. 2010; Ding et al. 2010; Tellefsen et al. 2012). They found that this shielding effect has a non-trivial relationship with the magnetic susceptibility of the fluid.

1.1 Objective

Even though magnetic contamination of drilling fluid has a proven adverse effect on the wellbore positioning, the lack of API or ISO standard for measuring this content is sensed. Knowing the magnetic contamination content of drilling fluids is occasionally important.

Therefore, this work aims to develop a measurement system to measure the weight of magnetic contamination of drilling fluid. An additional objective is to use the developed method to measure the weight of magnetic content of drilling fluid samples from a North Sea well. Finally, to evaluate the properties of the magnetic contamination, the microstructure of the collected content is analyzed using a Scanning Electron Microscope (SEM) and X-Ray Diffraction Analysis (XRD).

2 Literature Review

2.1 Why Should We Remove Magnetic Material from the Drilling Fluid?

Drilling fluids are used to facilitate the drilling operation and penetration of the formation. The main function of drilling fluid includes controlling formation pressure that might cause kick in the worst-case scenario, hole cleaning and transporting the cuttings from wellbore to the surface to avoid stuck pipe, transferring the heat from the bit to the surface and cool it, lubricating the well which extends the life of the bit, transferring hydraulic energy to the bit and protecting the wellbore stability. Initial drilling fluid is designed to meet certain requirements based on the formation, environmental, and economic concerns. The properties of drilling fluid then change when it circulates in the wellbore. Therefore, it is needed to monitor the character of the drilling fluid and refresh it by adding fresh drilling fluid. The mud engineer is responsible for monitoring the drilling fluid and measure the properties such as density, viscosity, filter loss, solid content, pH, etc. to ensure that the drilling fluid maintains its functionality.

As mentioned, one of the functions of the drilling fluid is to provide a medium to carry the cuttings to the surface when the bit penetrates the formation. Moreover, the drilling fluid carries magnetic materials such as metallic swarf and finer steel particles that stem from casing erosion, especially when the contact between the casing and the drill pipe increases or pipe abrasion due to barite transferring happens (Saasen et al. 2001). Naturally occurring minerals such as magnetite are also another source of magnetic materials that enters the drilling fluid when the formation is drilled. Finally, additives like barite, bentonite (contains up to 10% Fe_2O_3), hematite, etc. have some negative magnetic effects. The role of the magnetic debris present in the drilling fluid on shielding the earth's magnetic field and thus causing errors in the azimuth measurements has been well studied (Saasen et al. 2020; Wilson and Brooks 2001). Another drawback associated with magnetic particles in the drilling fluid is that they might damage the mud pump inner parts such as piston and liner (compression cylinders) because of the high abrasion (Saasen et al. 2019).

These steel particles also tend to agglomerate on the downhole tools and BOP. Thus, causing tool failure and rig downtime, which can be extremely expensive, specifically in offshore operations where the daily cost is very high (Saasen et al. 2019). Furthermore, if BOP,

which has the role of ensuring the well safety, fails to function normally, the outcome would be devastating.

It was reported that after removing the magnetic contamination of the drilling fluid, the signal to noise ratio of the Nuclear Magnetic Resonance (NMR) measurements was improved to a great level (Strømø et al. 2017). NMR technology has been used in downhole logging tools to obtain pore fluid and pore properties. The NMR logging tool has a magnet that produces a magnetic field in the downhole, and the hydrogen protons in the formation pore fluid align themselves when placed in the applied field, hence creating a magnetic moment. The NMR tool measures the magnetic released signal of the particle. Magnetic contamination in the drilling fluid might interrupt these emitted signals and produce noise.

2.2 Directional Drilling Challenges – Error Sources

2.2.1 Wellbore Surveying

Wellbore surveying is fundamental when drilling a directional well. Getting information of the wellbore position, such as inclination and azimuth, gives the opportunity to hit the target and maximize the production and avoid the collision between wells, which has catastrophic consequences. Also, knowing the well's accurate position helps a lot if the plan is to drill a relief well because drilling such wells demand high control on the well path. These well trajectory measurements are typically carried out every 30 meters.

Every invention begins with a problem or a need; wellbore surveying started in the early 20th century because the wells in that time had a high deviation from the planned vertical trajectory and caused some serious problems. One of the earliest inventions was the acid bottle, which was not so complicated. The instrument was run with a wireline, and it was left in the downhole to let the acid surface displace and left some marks on the bottle. Using some simple mathematic calculations, the inclination angle could be obtained. Moreover, a compass needle was used to find the azimuth of the well (Griswold 1929; Inglis 1987). Later, an instrument was introduced which used a camera to take a photograph of the magnetic compass and angle unit in the bottom hole. With this fast and straightforward survey operation known as "Single shot", the possibility of controlling the direction and inclination of the borehole was provided. This survey was run every 100 ft to get the well's accurate position (Eastman 1937; Hughes 1935).

The multishot survey followed the same principle as a single shot, but it took several photographs at specific time intervals instead of taking just one picture at each run. One of the advantages of this method was reducing the time needed to survey the well because this method gave the possibility of surveying the whole well in a single operation (Inglis 1987). A detailed description of this survey system and the tool's performance can be found in Thorogood and Knott (1990).

Magnetic surveys are unreliable when adjacent wells are too close, especially in upper sections of multi-well platforms or surveying the cased hole. Thus, gyroscope surveying is a good option when there is concern about magnetic interference. The gyroscope tools are made up of up to three accelerometers and three spinning gyros. By measuring the earth's gravity field, accelerometers are able to find inclination and tool face angle. The rotor gyroscope measures the rate of the tool and the earth's rotation. However, gyro surveying is not economical and more important, the error of the gyro becomes higher when the well is drilled near the north or south pole due to the fact that the rotation rate of the earth is lower (Bang et al. 2009; Garza et al. 2010; Torkildsen et al. 2008). Nowadays, the most standard technology for surveying the directional wellbores is measurement while drilling (MWD), where information is measured at the bottom hole and transmitted to the surface via mud column as pressure pulse. Unlike wireline surveying techniques, there is no need to halt the drilling operation in MWD. This common practice saves rig time, which is crucial, particularly in an offshore environment where the platform's cost is high (Inglis 1987).

2.2.2 Magnetic Survey

MWD tools contain a magnetometer and accelerometers that measure the earth's magnetic field and gravitational field in three dimensions sequentially (Gooneratne et al. 2019; Gooneratne, Li, and Moellendick 2017). Figure 1 shows the configuration of a typical MWD tool.

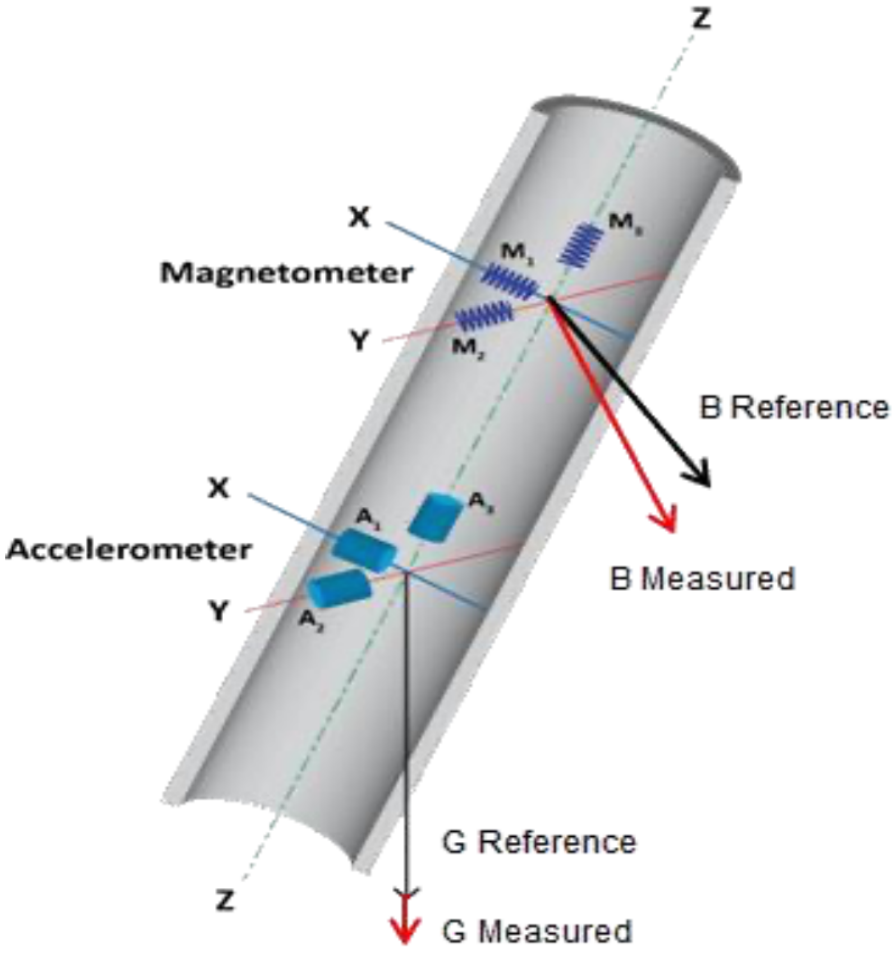

Figure 1 – Configuration of MWD tool. M and A represent magnetometer and accelerometer sensors along three axes in order (Stefan Maus et al. 2017)

The measurement from the accelerometer leads to the derivation of inclination and tool face angle when the well is drilled with deviation. With the help of this information and measurement from the magnetic compass, the azimuth of the well can be obtained (Edvardsen 2016). Earth's magnetic field and gravitational field vectors are:

$$B = \sqrt{B_x + B_y + B_z} \tag{1}$$

$$G = \sqrt{G_x + G_y + G_z} \tag{2}$$

The B_x, B_y and B_z components of the earth's magnetic field are measured by M_x, M_y and M_z sensors of fluxgate magnetometer. To convert these components from x-y-z coordinate system to north-east-vertical coordinate system, a transform matrix is used:

$$TM = \begin{bmatrix} \cos I \cos A \sin\alpha + \sin A \cos\alpha & \cos I \sin A \cos\alpha - \sin A \sin\alpha & \sin I \cos A \\ \cos I \sin A \sin\alpha - \cos A \cos\alpha & \cos I \sin A \cos\alpha + \cos A \sin\alpha & \sin I \sin A \\ -\sin I \sin\alpha & -\sin I \cos\alpha & \cos I \end{bmatrix} \quad (3)$$

$$\begin{bmatrix} B_N \\ B_E \\ B_V \end{bmatrix} = \begin{bmatrix} B\cos\theta \\ 0 \\ B\sin\theta \end{bmatrix} = TM \begin{bmatrix} B_x \\ B_y \\ B_z \end{bmatrix} \quad (4)$$

Solving for B_E leads to:

$$\begin{aligned} B_E = {} & (\cos I \sin A \sin\alpha - \cos A \cos\alpha)B_x \\ & + (\cos I \sin A \cos\alpha + \cos A \sin\alpha)B_y \\ & + (\sin I \sin A)B_z = 0 \end{aligned} \quad (5)$$

$$A = \tan^{-1} \frac{B_x \cos\alpha - B_y \sin\alpha}{\cos I \left(B_x \sin\alpha + B_y \cos\alpha\right) + B_z \sin I} \quad (6)$$

where A is azimuth, α is tool face orientation angle, θ is the dip angle, and I is the inclination. The G_x, G_y and G_z components of the earth's gravitational field are measured by A_x, A_y and A_z sensors of the accelerometer. dip angle can be found using:

$$\theta = \sin^{-1}\left[\frac{G_x B_x + G_y B_y + G_z B_z}{G.B}\right] \quad (7)$$

And inclination can be calculated by:

$$I = \cos^{-1}\frac{G_z}{G} \tag{8}$$

The toolface angle is divided into two categories: a) gravity toolface angle measured by accelerometer when the well has higher than 3° inclination b) magnetic tool phase measured by magnetometer when the well is drilled near vertical.

$$\text{Gravity toolface} = \tan^{-1}\frac{-G_x}{-G_y} \tag{9}$$

$$\text{Magnetic toolface} = \tan^{-1}\frac{B_x}{B_y} \tag{10}$$

2.2.3 Geomagnetic Field

There are three main origins that form the near surface earth's magnetic field vector measured by magnetometers. These sources that are shown in Figure 2 are the main field caused by the earth's liquid core, the crustal field generated by magnetic property of local rock (ferrous), and disturbance field due to solar activities in the magnetosphere (Akasofu and Lanzerotti 1975; Edvardsen et al. 2013; Poedjono et al. 2012).

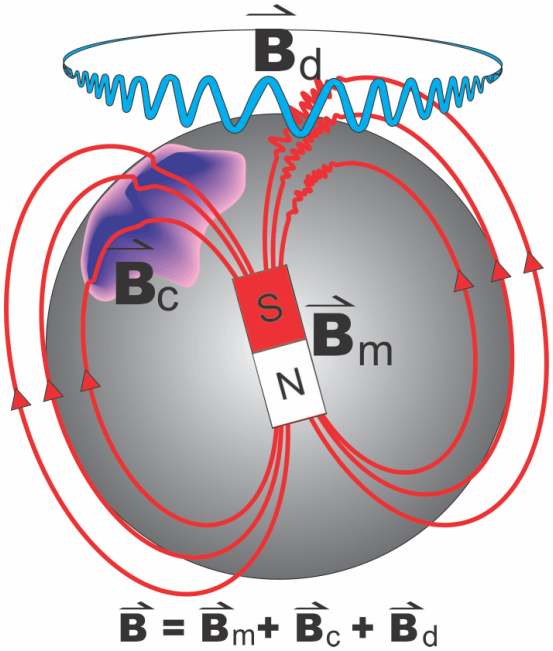

Figure 2 – Three field that forms the near surface geomagnetic field (Edvardsen 2016)

The near surface geomagnetic field B is identified by vector decomposition into the components, as shown in Figure 3. The total field can be expressed as a horizontal and vertical component. Dip angle is the angle between the total field and the horizontal plane. The magnetic borehole survey instrument measures azimuth with reference to the magnetic north, which needs to be converted to true geographic north because the magnetic north is not a stable reference and changes over time. An accurate reference model is needed to find the declination, which is the angle between the true north and geographic north.

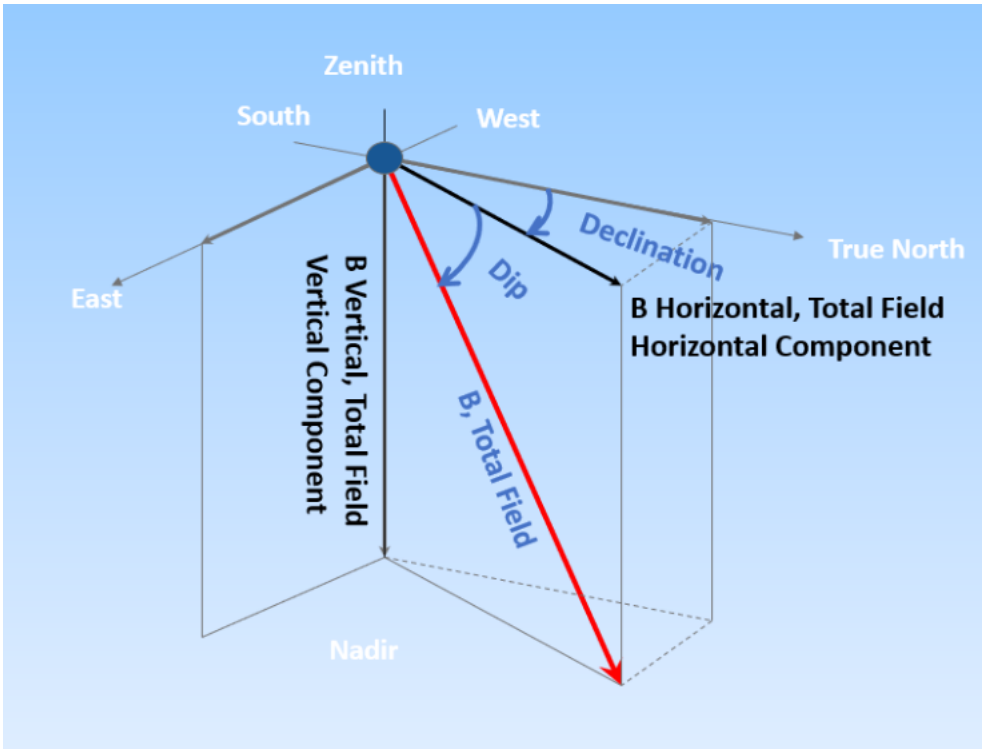

Figure 3 – Geomagnetic field components (Saasen et al. 2020)

The accuracy of the magnetic directional surveying is a function of the geographic latitudes, as demonstrated in Figure 4. The horizontal component of the geomagnetic field becomes smaller in high latitudes (dip angle increases), and errors in azimuth measurement increase. Thus, making the downhole surveying of the wellbore more challenging in the Arctic region and increasing the chance of collision with adjacent wells.

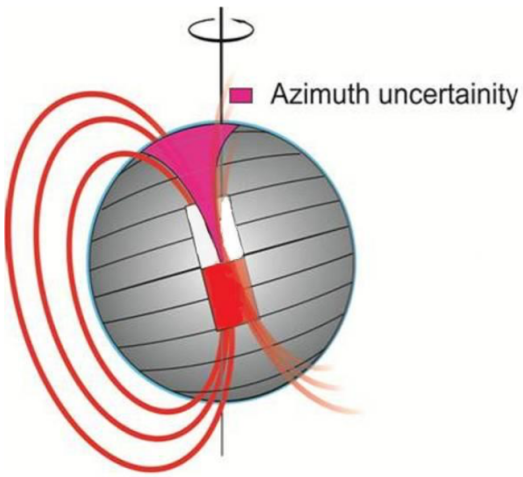

Figure 4 – Azimuth uncertainty and geographic latitudes

2.2.3.1 Geomagnetic Field Reference Model

To find the earth's magnetic field in any place on the earth, the real time reference model is used. The reference models that take into account the crustal field and disturbance field are more accurate. However, most of the models only consider the main field caused by the earth core. These models allow the measurement of the declination, dip angle, and total magnetic field along the well path, which are then compared to MWD tool measurements for quality check and converting the magnetic north to geographic north. Thus, choosing an accurate geomagnetic field model that covers local variation is vital (Poedjono et al. 2010). Some of the global magnetic field models used are International Geomagnetic Reference Field (IGRF) and BGS Global Geomagnetic Model (BGGM). The latter model is more accurate and used for directional drilling surveys (Buchanan et al. 2013; Edvardsen 2016).

2.2.4 Source of Errors in Azimuth Measurement

Drillstring with the magnetic properties, magnetic drilling fluid, magnetic interference of the neighbor well's casing, and the solar activities in high latitude region (north pole and south pole) makes the accurate measurement of the well path harder as they cause errors in the azimuth data which in a worst-case scenario may cause a collision with adjacent wells (Edvardsen et al. 2019; Wilson and Brooks 2001). The uncertainty in azimuth measurement increases when the well is drilled horizontally in the east (or west) direction. The available solutions to correct the magnetic drill string are multistation analysis (MSA) or using non-magnetic collars (non-magnetic spacing), which is not practical sometimes (Brooks, Gurden, and Noy 1998; Lowdon and Chia 2003).

The disturbance field due to electrical currents in the high geographic latitudes can make the geomagnetic reference model unreliable. The result is declination reference error which can be tackled using infield referencing (IFR). IFR technique is performed by observing the local magnetic field stations near the wells located in the Arctic or Antarctic. For the wells that are not close enough to the observation station, the interpolated infield referencing (IIFR) is advantageous where the interpolation of measurements of near observation stations are used (Kabirzadeh et al. 2018; Lowdon and Chia 2003; Williamson et al. 1998).

Besides the non-trivial effect of the magnetic drilling fluid in downhole surveying accuracy, there is no technique that takes into account this effect because of the dynamic nature

of the drilling fluid (Amundsen et al. 2010). Furthermore, the magnetic content of drilling fluid is not among the source of errors in the error model introduced by the Industry Steering Committee for Wellbore Survey Accuracy (ISCWSA) to quantify the ellipsoid of uncertainty (ISCWSA 2012). Accordingly, effective cleaning of the magnetic contamination of the drilling fluid remains the only solution.

2.3 The Role of Drilling Fluid in Shielding the Magnetic Field

It is well known that magnetic particles in the drilling fluid can negatively affect the directional wellbore positioning from both experimental works (Amundsen et al. 2010; Ding et al. 2010; Wilson and Brooks 2001) and surveying data (Saasen et al. 2020). It is good practice to first take a look at the theory of magnetic susceptibility to better understand how magnetic particles can shield the earth's magnetic field measured by downhole magnetic sensors.

2.3.1 Magnetic Susceptibility

One of the material's fundamental properties that define its ability to be magnetized in an applied magnetic field is magnetic susceptibility (Wightman, W. et al. 2004). It is the ratio of the magnetization to the magnetic field (Getzlaff 2008; Spaldin 2011):

$$\chi = \frac{\mathrm{M}}{\mathrm{H}} \tag{11}$$

where χ is volumetric susceptibility and dimensionless in SI unit. There are also other measures of susceptibility. For instance, mass susceptibility is obtained by dividing the volumetric susceptibility by density with unit $\mathrm{m^3kg^{-1}}$in SI.

Another property is permeability, which shows the degree of material magnetization when it is exposed to the magnetic field:

$$\mu = \frac{\mathrm{B}}{\mathrm{H}} \tag{12}$$

where B is magnetic induction (magnetic field vector) and H is applied magnetic field. The magnetic induction relates to the magnetic field with the following formula:

$$B = \mu_0(H + M) \tag{13}$$

where μ_0 is the permeability in a vacuum.

With the help of equations *11* and *12*, The relation between magnetic susceptibility and permeability is as follows:

$$\frac{\mu}{\mu_0} = 1 + \chi \tag{14}$$

Drilling fluid consists of several components such as weighting agent, viscosity controller, filter loss additives, etc. Therefore, to find the susceptibility of the drilling fluid, one can use Wiedemann's law for the susceptibility of a mixture (Bakker and de Roos 2006; Kuchel et al. 2003):

$$\chi(\text{mixture}) = \frac{\sum_{i=1}^{M} V_i \chi_i}{\sum_{i=1}^{M} V_i} \tag{15}$$

where V_i and χ_i are the volume and the susceptibility of component *i* in the mixture. However, the mentioned law is not entirely acceptable because it does not consider the chemical interaction between components in the mixture.(Giorgio Pattarini 2015; Kuchel et al. 2003).

Another mixing formula belongs to Maxwell-Garnett, which gives effective permeability of the mixture containing spherical particles (Giorgio Pattarini 2015; J. C. Maxwell Garnett 1904):

$$\mu_{eff} = \mu_2\left(1 + \frac{3\delta(\mu_1 - \mu_2)}{\mu_1 + 2\mu_2 - \delta(\mu_1 - \mu_2)}\right) \tag{16}$$

where δ is the volume fraction of the particles in the fluid, and μ_1 and μ_2 are permeability of the particle and medium (fluid), respectively. Finally, it leads to the effective susceptibility of the mixture:

$$X_{eff} = \frac{\mu_{eff} - \mu_0}{\mu_0} = \frac{3\delta X}{3 + X(1 - \delta)} \quad (17)$$

2.3.2 Magnetic Particles

2.3.2.1 Diamagnetism

In a diamagnetic substance, atoms have zero magnetic moments. However, when exposed to the magnetic field, it shows negative magnetization. In other words, magnetic moments in this substance orient themselves antiparallel to the applied magnetic field. Lenz's law can describe this phenomenon. Therefore, it is obvious that these materials' magnetic susceptibility is negative and independent of temperature (Cullity and Graham 2009; Getzlaff 2008). Table 1 shows the values for some of the diamagnetic material (Tarling and Hrouda 1993).

Table 1 – Magnetic Susceptibility of diamagnetic materials

Material	Mean volumetric susceptibility (dimensionless in SI unit) at room temperature
Dolomite	-38×10^{-6}
Quartz	-13.4×10^{-6}
Calcite	-13.8×10^{-6}
water	-9×10^{-6}

2.3.2.2 Paramagnetism

In Paramagnetic material, unlike diamagnetic, atoms show net magnetic moment, and when placed in an applied magnetic field, the atomic moments tend to align themselves toward the magnetic field. Hence, the magnetization and susceptibility are positive. In this type of material, when the field is removed, the magnetization becomes zero. In other words, magnetization is temporary. Table 2 shows the mass susceptibility of paramagnetic minerals. Note that the values are in 10^{-8} m^3kg^{-1}. As shown in Figure 5, in both diamagnetic and paramagnetic material, magnetization is a linear function of an applied field.

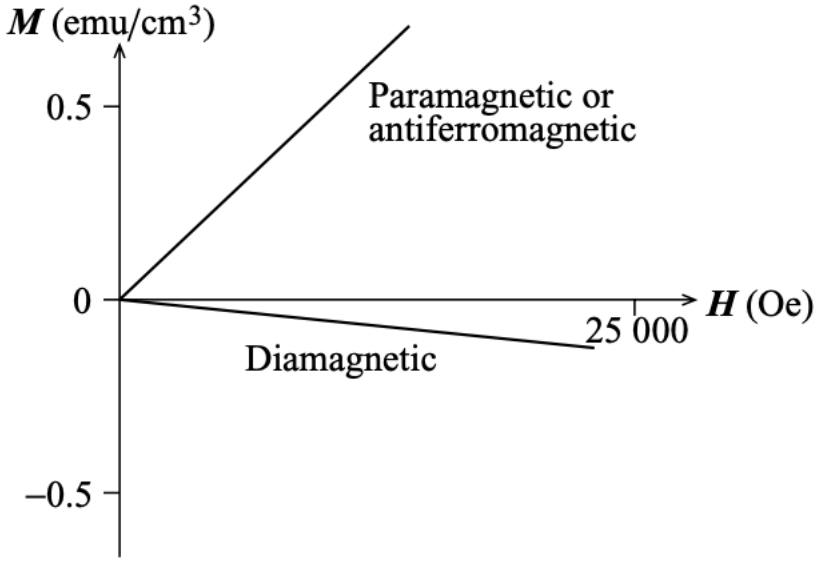

Figure 5 – Magnetization as a function of applied field for diamagnetic and paramagnetic materials (Spaldin 2011)

Table 2 – Magnetic Susceptibility of paramagnetic materials

Mineral	Mass susceptibility (10^{-8} m^3kg^{-1} SI unit) at room temperature
Pyrite	1-100
Chlorite	358
Muscovite	165

Bentonite	5.8
Ilmenite	170-200

2.3.2.3 Ferromagnetism

Ferromagnetic materials are spontaneously magnetized without an applied field. However, they exhibit strong magnetization in the presence of the field. Steel swarf is believed to be in this category. The susceptibility of this type of material is dependent on temperature. Thus, it makes the measurement harder for drilling fluid that circulates through the downhole and has a high temperature. Table 3 shows the mass susceptibility of the magnetite and hematite (Zawadzki and Bogacki 2016).

Table 3 – Magnetic Susceptibility of ferromagnetic materials

Mineral	Mass susceptibility ($10^{-8}\ m^3kg^{-1}$SI unit) at room temperature
Magnetite	20000-110000
Hematite	10-760

2.3.3 Magnetic Shielding

As described earlier, magnetic susceptibility indicates how much the material, which is drilling fluid in this case, can be magnetized when exposed to a magnetic field. Consequently, magnetic particles orient themselves according to the magnetic field and attenuate the intensity of the field measured by the magnetic sensor. To give numbers for drilling fluid, susceptibility higher than χ =0.01 (in SI) is considered the problem (Amundsen et al. 2010). Magnetic susceptibility of material is measured with well-known methods like Guoy's scale and Faraday's scale or by the help of SQUID magnetometer (Marcon and Ostanina 2012). However, measuring the susceptibility of the drilling fluid is not routine since it has dynamic properties, and the circulation of drilling fluid in the wellbore is a contributor to this issue as well (Saasen et al. 2016).

Amundsen et al. modeled the shielding of the earth's magnetic field measured by magnetic sensors (Amundsen, Torkildsen, and Saasen 2006). They assumed a simple case where the magnetometer is located on the axis of the wellbore that is filled with drilling fluid with magnetic susceptibility χ. Based on these assumptions, they found that the magnetic field can be shielded to a factor of $\frac{1}{4}\chi^2$. This shielding factor, however, cannot justify the observed attenuation during some directional drilling surveys. For instance, the mentioned equation gives a dampening of 0.1% when the drilling fluid with a typical value of susceptibility of 0.063 is used in the well. The survey data set provided by Torkildsen et al. showed that the damping of the magnetic field could be 2.6 % for oil-based drilling fluid (OBDF) (Torkildsen et al. 2004). Another work that simulated a more complex situation with the finite-element method (FEM) concluded that the wellbore geometry is also a contributor to the complexity of measurement (Waag et al. 2012).

The magnetic drilling fluid mainly disrupts the sensor measurements perpendicular to the axis (x-y) while the drillstring distorts the axial measurements. Figure 6 shows this concept in a schematic way. The magnetic debris of the drilling fluid can finally produce 1-2 degrees of error in the azimuth measurement (Amundsen et al. 2006; Torkildsen et al. 2004; Wilson and Brooks 2001).

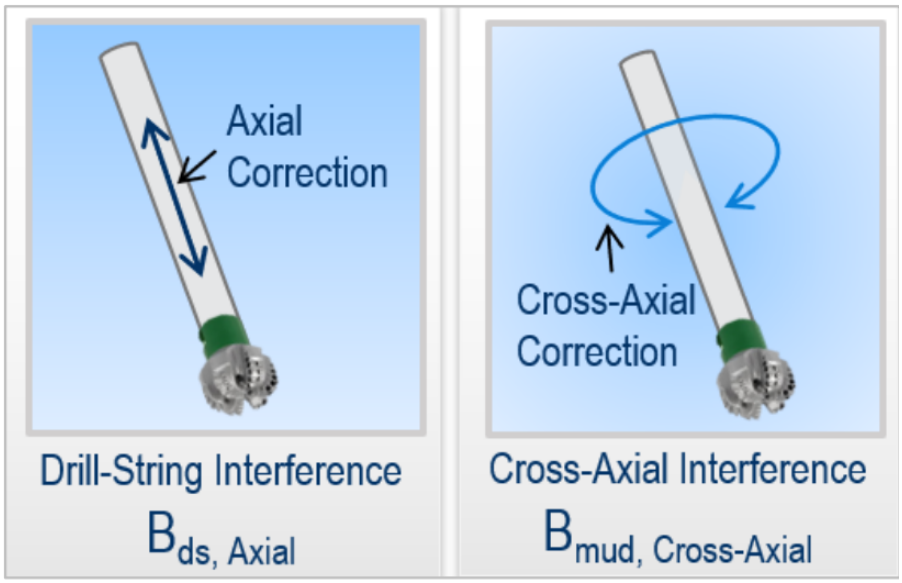

Figure 6 – Drillstring and drilling fluid magnetic interference (Saasen et al. 2020)

2.3.4 Type of the Drilling Fluid Additives and Magnetic Shielding

2.3.4.1 Magnetite

Ding et al. utilized an experimental approach to observe the magnetic shielding phenomenon induced by drilling fluid (Ding et al. 2010). By adding magnetite powder to the xanthan gum and water solution, which is a non-Newtonian shear-thinning fluid, they observed that the earth's magnetic field measured by fluxgate magnetic sensor that was immersed into the prepared fluid could be attenuated to a high degree. They used magnetite powder with susceptibility of 2.0 to reproduce the magnetic content of the weight additives in the drilling fluid. Figure 7 shows the result for the various concentration of the magnetite in the drilling fluid and dynamic shielding of the field. Further, they investigated that low viscosity of the fluid has two different impacts on the shielding: a) it allows the particles in the fluid to orient easier and increase the attenuation b) magnetic particles settle out easier, and thus faster reduction in the attenuation takes place (Ding et al. 2010).

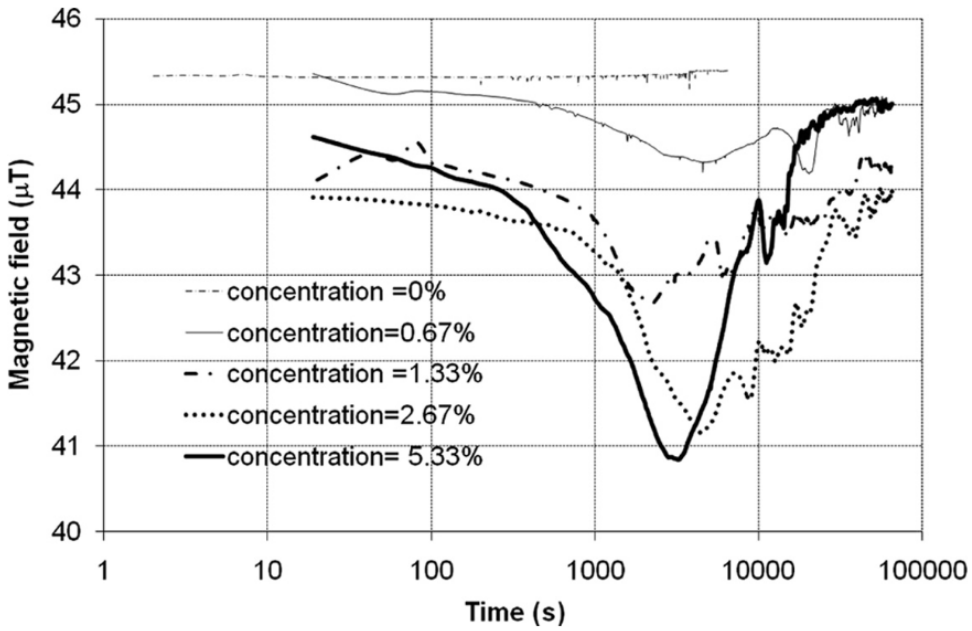

Figure 7 – Magnetic shielding of magnetite (Ding et al. 2010)

It was found by Amundsen et al. that there is a relation between the size of the magnetic particles and the magnetic shielding (Amundsen et al. 2010). For the finer particles, the viscous force is dominant over the magnetic force; thus, a slower dampening of the magnetic field

happens. On the other hand, the coarser particles tend to sag earlier, and rapid recovery of the magnetic field from the minimum can be seen.

2.3.4.2 Bentonite

Bentonite is one of the common additives of water-based drilling fluid (WBDF) and improves rheological behavior and filtration control. To observe the effect of the bentonite on the magnetic field measured by the MWD tool, the varying concentration of bentonite was added to simple WBM (Tellefsen et al. 2012). As it is demonstrated in Figure 8, the reduction in the measured magnetic field is a function of the bentonite concentration. Contrary to the magnetite, here, the dynamic behavior of the measurement as a function of time could not be seen. High concentration of bentonite in the mixture develops an unsteady structure that prevents any rotation of particles. Hence, we do not see very significant dynamics in shielding.

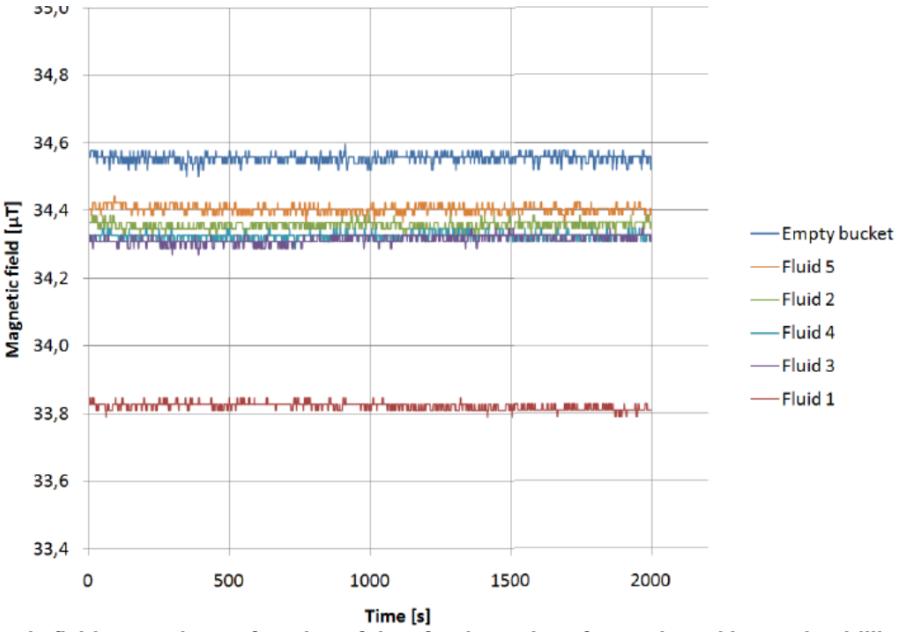

Figure 8 – Magnetic shielding of bentonite (Tellefsen et al. 2012)

2.3.4.3 Organophilic Clay

The presence of hectorite as organophilic clay in the OBDF has no link with magnetic shielding since it has low iron content in the composition. However, other types of organophilic clay should be investigated (Tellefsen et al. 2012).

2.3.4.4 Swarf

Most of these coarse magnetic particles are normally removed from drilling fluid by ditch magnets and distinguished from the finer magnetic particles. Based on the research done by the Tellefsen et al. , it was found that swarf significantly reduced the magnetic field measured by the magnetometer that was immersed inside the drilling fluid (Tellefsen et al. 2012). The measured reduction was from 34.49μT to 26.14μT, and the dynamic behavior observed with magnetite was also observed here.

2.3.4.5 Weight Material

The susceptibility measurement of the barite and ilmenite as two common weight materials was conducted by Torkildsen et al. it indicates a higher value for ilmenite than barite. In addition, several survey data set were analyzed and showed a higher magnetic shielding for the drilling fluid that had ilmenite which again confirms the experiment results (Torkildsen et al. 2004).

2.4 Ditch Magnets and Removing the Magnetic Contamination of Drilling Fluid

The oil and gas industry's response to the challenge of magnetic drilling fluid was the invention of the ditch magnet system. Dich magnets system consists of robust magnets that can be configured vertically or horizontally. Usually, the ones with vertical magnetic rods are more efficient than those with horizontal magnets lying in the bottom of the flowline (Saasen et al. 2019). Ditch magnets are commonly located before or after the shale shakers; thereby, the drilling fluid that returns from the downhole and goes through the mud return line passes through them. To get information about various type of ditch magnets, it is recommended to read the work done by Strømø et al. (Strømø 2016). The performance of the ditch magnets in removing the magnetic contamination of drilling fluid highly depends on the system's design. Flow-positioned ditch magnet system efficiency in removing the magnetic particles was reported by a couple of works (Pattarini et al. 2017; Saasen et al. 2019; Strømø et al. 2017). This system has a flow director to drive the fluid as near as possible to the magnets. Thus, enables the magnet to collect finer magnetic particle since the magnetic force overcomes the drag force in this way. The flux density of the magnet indicates that the magnetic force reduces

to half when the distance from the surface of the magnet is higher than 5 mm. Data of magnetic contamination cleaned from the magnet was extracted from the daily drilling report of the wells drilled with Maersk Interceptor in Ivar Aasen field and other wells drilled with a semi-submersible drilling rig. The former set of wells were equipped with Flow positioned ditch magnets, and later wells were equipped with a conventional type of ditch magnet. It is obvious from Figure 9 that this new type of ditch magnet was more successful in removing the magnetic particles, especially finer ones that are believed to have a significant role in producing errors in azimuth measurement (Strømø et al. 2017).

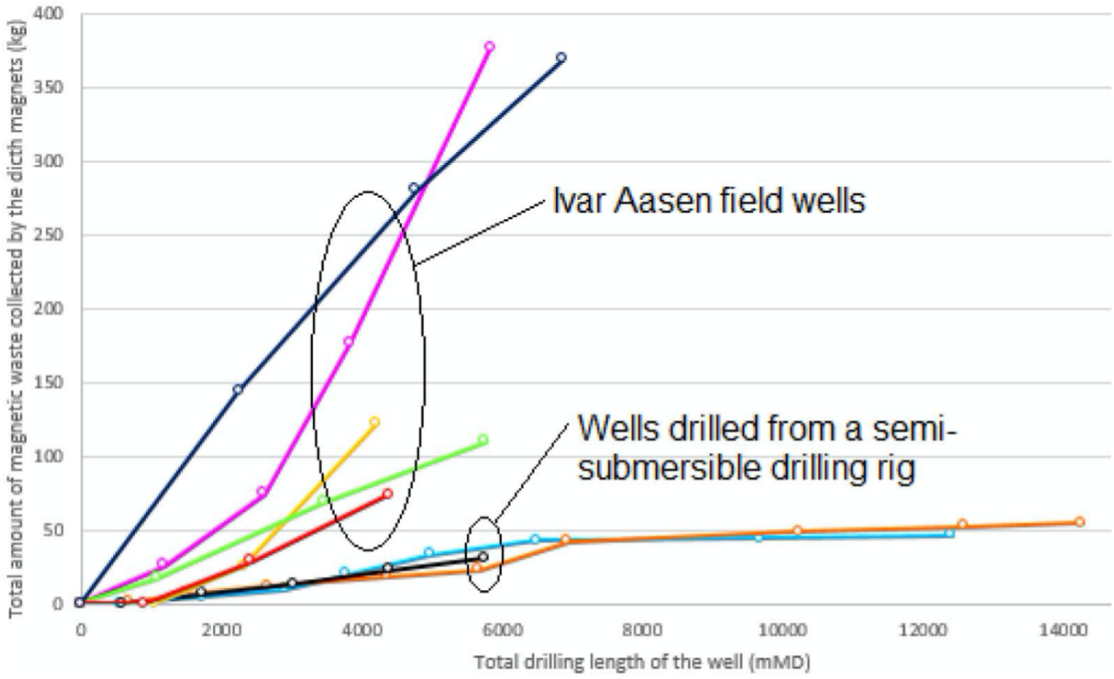

Figure 9 – Performance of flow positioned ditch magnet compared to conventional ditch magnet (Saasen et al. 2020)

The horizontal and vertical component of the earth's magnetic field measured by the downhole magnetic sensor of Ivar Aasen field's well was compared to the geomagnetic reference model values (Saasen et al. 2020). Figure 10 demonstrates the difference in the values, and the 0 value in both axes represents the high accuracy of the measurements. The dashed line rectangle is the quality box, and the measurement points that fall inside it have an acceptable quality according to the Ivar Aasen field criteria. It shows that after magnetic cleaning of the drilling fluid with Flow positioned ditch magnet, the accuracy of the directional survey increases greatly.

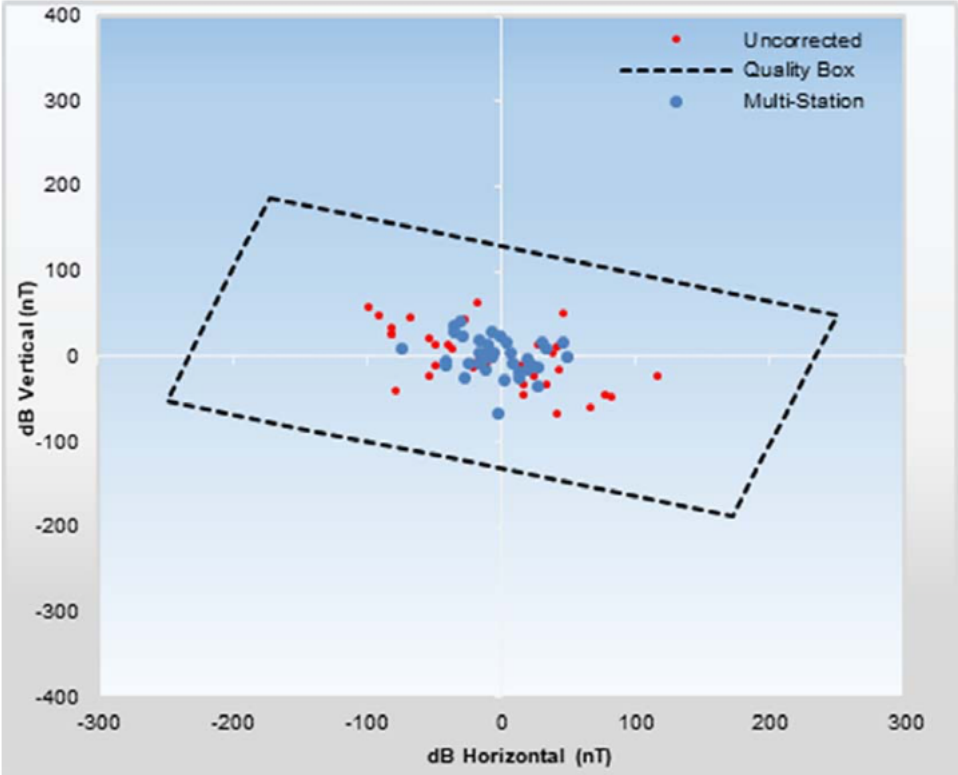

Figure 10 – Accuracy of wellbore survey at Ivar Aasen after removing the magnetic contamination of drilling fluid (Saasen et al. 2020)

3 Methodology

In this chapter, in the first step, a short description of the general equipment used in the laboratory and the advanced instrument used to analyze the microstructure of magnetic material collected from the drilling fluid are provided. A setup that is designed to fulfill the objective of this work is presented. This chapter also covers the details of the measurement system that was utilized to measure the magnetic content of the drilling fluid. Afterward, the ingredient used to prepare the model drilling fluid is described.

3.1 Equipment

3.1.1 Mettler Toledo Scale

Model MS104S was used to measure the weight of the collected magnetic material. The Readability of this scale is 0.1 mg. Figure 11 shows the scale used in this work. The accuracy of the measurement is of great importance; that is why this specific type of scale was employed.

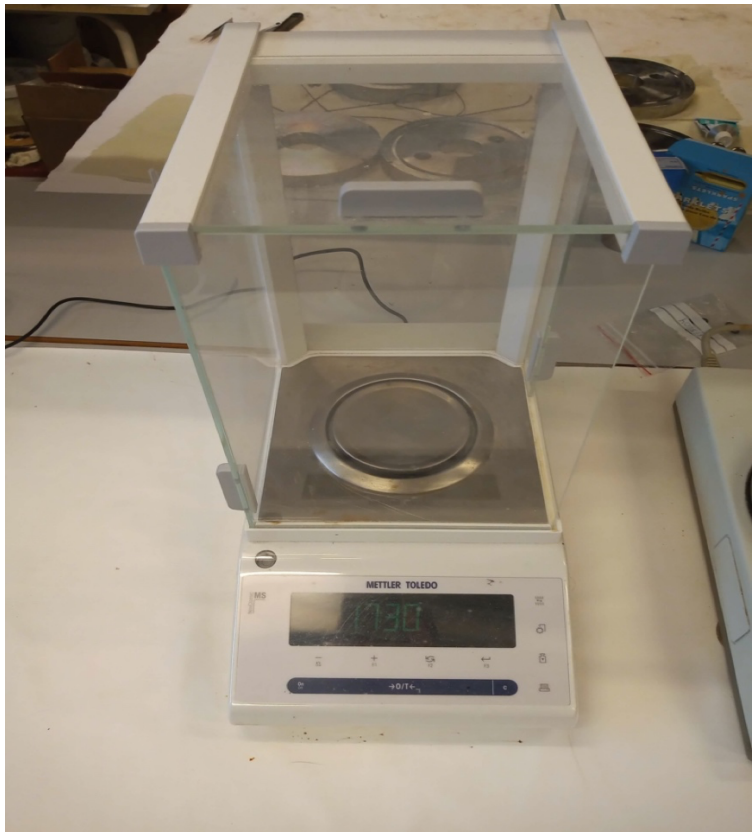

Figure 11 – Mettler Toledo Scale

3.1.2 Hei-TORQUE Value 400

It is used to prepare the model drilling fluid and mix the additives. This blender is able to produce up to 2000 rpm speed of rotation. The stirring tool that was used is a ringed pitched-blade impeller with an 8 mm stirrer shaft and 33 mm agitator.

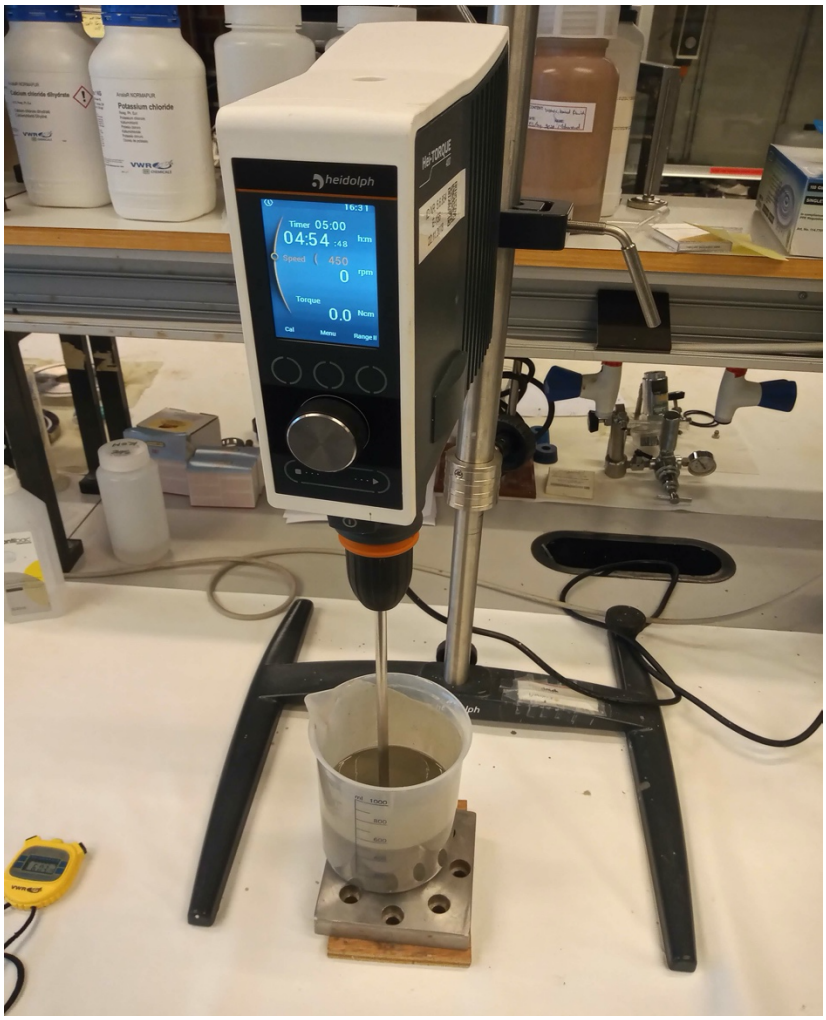

Figure 12 – Hei-TORQUE Value 400

3.1.3 Viscosity Measurement

The viscosity of the drilling fluids was measured with OFITE 900 rotational viscometer in accordance with recommended practice proposed by API at room temperature. Shear stresses correspond to 600,300,200,100,6, and 3RPM standard fixed shear rates were

measured. A conversion factor of RPM × 1.703 = 1/s and $\frac{\text{lb}}{100\text{ft}^2} \times 0.4788 = \text{Pa}$ for shear rate and shear stress were used respectively.

Figure 13 – OFITE 900 rotational viscometer

3.1.4 X-Ray Diffraction Analysis (XRD)

XRD Bruker D8 Advance was used to analyze the collected magnetic material and determine the material's crystallographic structure. The specimen is exposed to striking X-rays produced by a cathode ray tube, and then strength and reflected angles of the X-rays from the material are measured by a detector. The diffraction pattern of the X-ray gives information about the characteristics of the material under investigation. Braggs's law describes the relationship between the wavelength of radiation to the diffraction angle and spacing between diffracting planes in a crystalline sample:

$$n\lambda = 2d \sin \theta$$

where θ is diffraction angle, λ wavelength of beam, and d is the distance between diffracting planes. X-ray diffractogram of the specimen is measured in the step of 0.01 degree from 10 to 100 degrees (Patel and Parsania 2018).

3.1.5 SEM

One of the commonest instrumental methods to characterize and examine the micro and nanoscale particles is the Scanning Electron Microscope (SEM). This test was performed using Zeiss Supra 35 VP. An EDAX detector was used For Energy dispersive x-ray spectroscopy (EDS). This technique gives an estimation of the composition of the sample by sending an electron beam on the near surface of the sample and measuring the x-rays that particles emit when the beam penetrates the depth of the sample. Elemental analysis on the nanoscale area is the ability of this method.(Shukla and Iravani 2019; Welker 2012). Figure 14 shows the SEM setup that was used in this study.

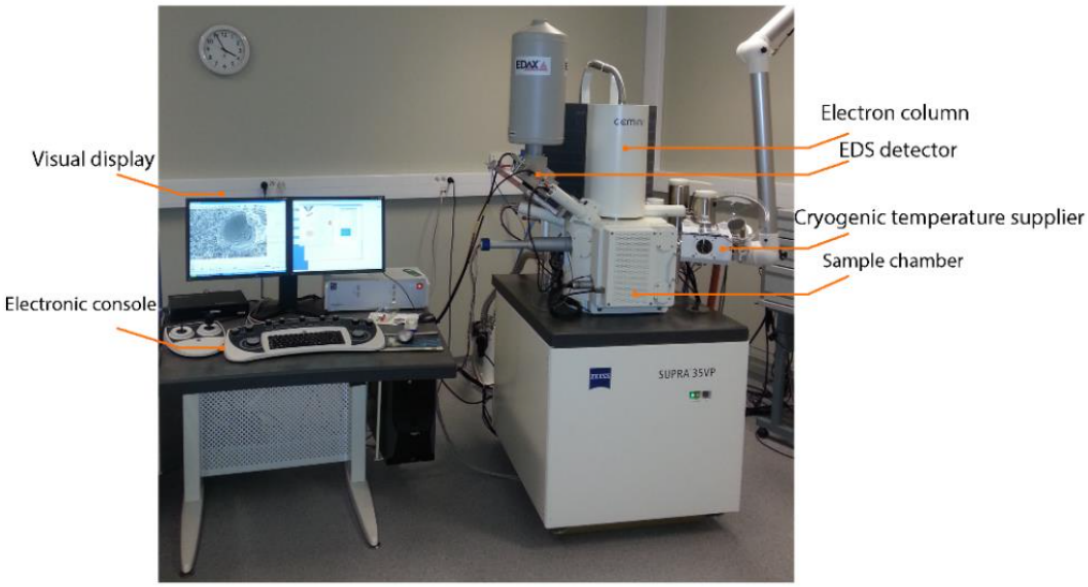

Figure 14 – SEM test setup (Mahmoud Khalifeh 2016)

3.2 Setup and Measurement System

In this work, a powerful magnetic rod, which was provided by Jagtech, was used to capture the magnetic content in the drilling fluid. This magnet was built as a stack of Neodymium magnets and is the strongest type of permanent magnet available commercially (Fraden 2010) and is usually used in the ditch magnet system. A minor modification was carried out to make the handling of the magnet easier. Magnetic flux density, which is tesla in SI unit, measured at different distances from the magnet, is shown in Figure 15. It indicates that the magnetic field approximately cuts down to one-third at 5mm millimeters distance from the magnet, and thus particles that are close enough can be attracted to the magnet.

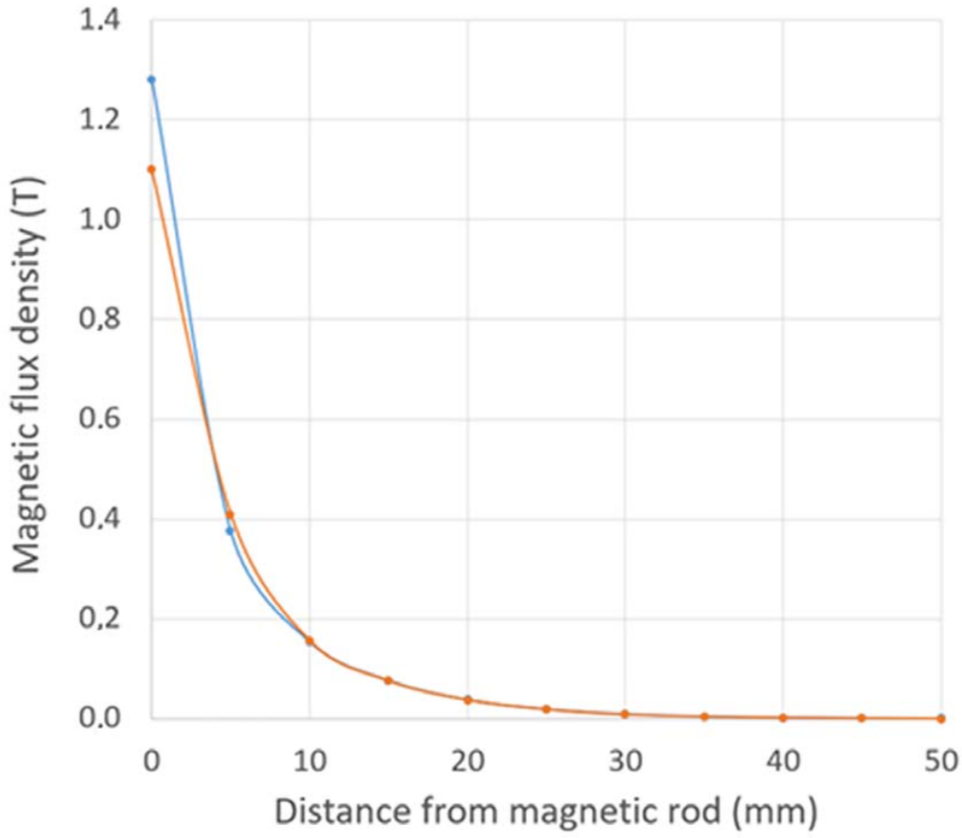

Figure 15 – Magnetic flux density measured at different distances from the magnet surface

A glass tube was used to protect the magnet from magnetic particles and avoid direct contact between them since removing the magnetic materials from the magnet is not easy and

may cause some errors in the measurements. However, the inner diameter of this glass tube should be approximately the same size as the outer diameter of the magnet to minimize the loss of the magnetic force, knowing the fact that the magnetic field is highly dependent on the distance from the magnet. In our experiment, the inner diameter of the glass tube and outer diameter of the magnet were 27 mm and 25 mm respectively. In general, a glass tube with a small thickness is preferred. The magnetic particles move from the glass tube to the magnet itself when trying to pull the magnet out of the glass tube, which might cause some problems. Accordingly, a 3D-printed plastic object (barrier) was tightened to the glass tube to block the movement of the magnetic particles. Figure 16 is the infographic of the setup that was used to collect the magnetic content of the drilling fluid.

Figure 16 – Simple equipment that was used to measure the magnetic content of drilling fluid

The measurement system steps to measure the weight of magnetic content were as follows:

1- The procedure started with mixing the drilling fluid to make sure that magnetic particles dispersed uniformly and filling 500 ml of drilling fluid sample into 1000 ml beaker for testing.

2- Immersing the magnet while it was placed in the glass tube into the drilling fluid sample.

3- Afterwards, the magnet was stirred in a circular pattern for 60 seconds in the drilling fluid and pulled out of the drilling fluid after stirring (Figure 17).

4- The magnet and the glass tube were gently shaken to ensure no additional drilling fluid filtrate was attached to the glass tube.

5-The magnet was pulled out of the tube, and the contents (magnetic and non-magnetic) attached to the tube were moved to another beaker and diluted by adding the water (base fluid) to reduce the residual concentration such as drilling fluid filtrate, polymers, and other non-magnetic particles

6- Again, the glass tube with the magnet was immersed in the diluted fluid and stirred for few seconds to collect all the magnetic particles. The adhered particles to the glass tube were dislodged by rinsing and transferred to the weighing dish and left to dry and evaporate the water content in the oven at 50 ℃ for two days.

7- Finally, the mass of the dry extracted magnetic debris (still some non-magnetic exist) was measured with scale (Figure 18).

From now on, for better understanding, we call the above-described steps the magnetic extraction. Magnetic extraction was repeated multiple times on a single drilling fluid sample until getting the same mass of content which shows that no magnetic contamination is left in the drilling fluid and only non-magnetic content stick to the glass tube. However, it is not possible to know the weight of the dry collected content in each extraction before using the oven. Therefore, it is recommended to place the magnet in the drilling fluid and repeat magnetic extraction a minimum of eight times to get complete results.

Figure 17 – Steps 2 and 3 of the measurement system

Figure 18 – Steps 6 and 7 of the measurement system

3.3 Model Drilling Fluid

The model drilling fluid was prepared to observe the performance of the magnet in attracting the magnetic particles. The experiments in this work were conducted using the water-based system because in this type of drilling fluid gel strength is higher comparing to OBDF, and gel strength acts against the magnetic force (Saasen et al. 2002). This is beneficial for the experiment as the high gel strength simulates the worst-case scenario and diminishes the efficiency of the magnet.

The simple modeled drilling fluid consists of a high amount of Xanthan biopolymer to increase the fluid's viscosity and prevent sagging of the heavy particles. Steel powder was used to introduce magnetic particles into the drilling fluid. The full composition of the model drilling fluid and mixing time are shown in Table 4. A Heidolf Torque 400 mixer was used to mix the ingredient and prepare the drilling fluid.

Table 4 – Mix design of model drilling fluid

Ingredients	Quantity (g)	Mixing time (min)
Tap water	500	NA
Xanthan biopolymer	4.3	10
Steel powder	1	15

3.3.1 Steel Powder

Steel powder with the apparent density of 2.96 g/cm3 and the particle size distribution that is shown in Table 5 was used to introduce magnetic particles into the model drilling fluid. The reason behind choosing the powder with this particle size range was to simulate the real magnetic debris present in the drilling fluid caused by casing and pipe corrosion. The composition of the steel powder provided by the manufacturer given in Table 6 indicates that steel powder is made of 97 % iron.

Table 5 – Size distribution of steel powder particles used in model drilling fluid

Size (Micrometers)	>250	250-150	150-45	45<
Percent %	negligible	11	65	24

Table 6 – Chemical composition of the steel powder (provided by the supplier)

Composition	Fe	Mo	Ni	Mn	O
Weight%	97.33	0.56	1.83	0.15	0.13

4 Result and Discussion

4.1 Model Drilling Fluid

Several works investigated the effect of magnetic particles present in the drilling fluid that are generated from various sources on the shielding of the magnetic field. However, the lack of a repeatable measurement system to measure the weight of magnetic content of the drilling fluid is sensed as there is no recommended practice for this purpose in API (American Petroleum Institute 2014) and ISO (International Organization for Standardization: Petroleum and Natural Gas Industries 2008).

The model drilling fluid with the ingredients mentioned in the methodology section (Table 4) was prepared, and the weight of the magnetic content was measured in each magnetic extraction mentioned in the previous section. Magnetic extraction was performed eight times, and each time, the magnet was stirred for 60 seconds in the drilling fluid. This was done to see if there is any correlation between the number of extraction and the amount of collected magnetic content which finally helps us estimate the total weight of magnetic contamination in the drilling fluid sample. The magnetic force exerted on the magnetic particles is proportional to the volume and the susceptibility of the particle, and the intensity of the magnetic field (Ge et al. 2017). Figure 19 shows the measured magnetic content after each magnetic extraction from the model drilling fluid. The weight of collected magnetic particles decreased as we repeated extraction with the magnet on the same drilling fluid, and the measured weight tended to zero at large numbers. This might be an indication of the effectivity of the magnet in attracting the magnetic particles, and there is not much magnetic content left in the sample drilling fluid after eight times magnetic extraction. On the other hand, when we collected the magnetic content of the drilling fluid, there was a small portion of polymer sourced from Xanthan gum that was also attached to the glass tube (magnet was placed inside) and made the weight measurement less accurate. The high concentration of the Xanthan gum and thus high viscosity of base drilling fluid believed to be a contributor to this issue. Another phenomenon that adds to the complexity of the measurement is rusting, which is due to the oxidation of iron atoms.

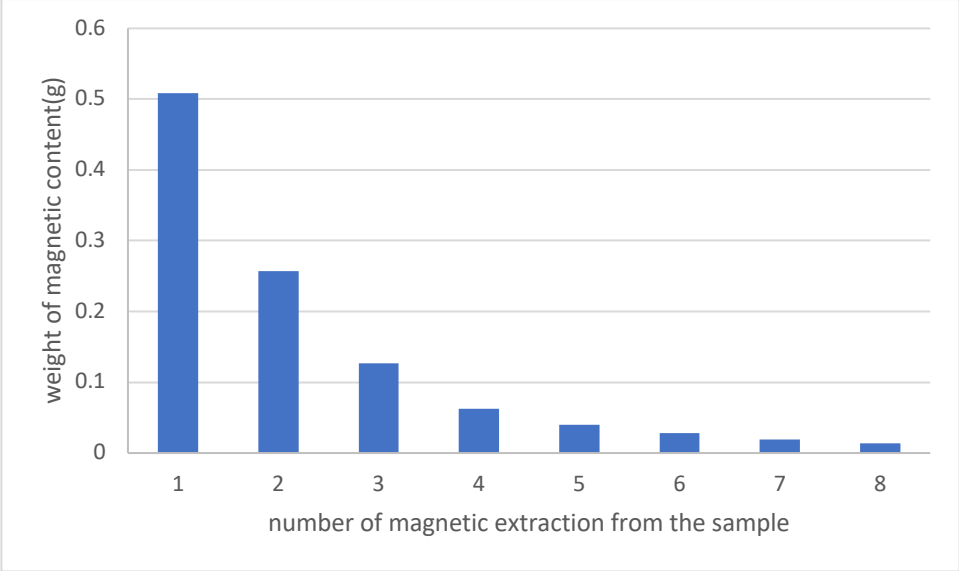

Figure 19 – Measured magnetic content of model drilling fluid after eight magnetic extraction

The total magnetic content of the model drilling fluid measured after eight magnetic extractions was 1.0551 grams, although we added 1 gram of steel powder to the model drilling fluid in the preparation process. On this account, oxidation of iron and presence of polymer in the so-called magnetic content have added to the uncertainty of measurement.

On this account, there was a small amount of polymer also in the so-called magnetic content and oxidation of iron added to the measured weight. The performance of the magnet in attracting the magnetic content is highly dependent on the viscosity of the drilling fluid, the size of the magnetic particles, the distance from the magnet, and more importantly flux density of the magnet. However, it is expected that if a magnet with a different flux density is used, the same reduction trend as Figure 19 will be observed. This can be an interesting subject for future works. Figure 20 shows the picture of the magnetic particles collected each time.

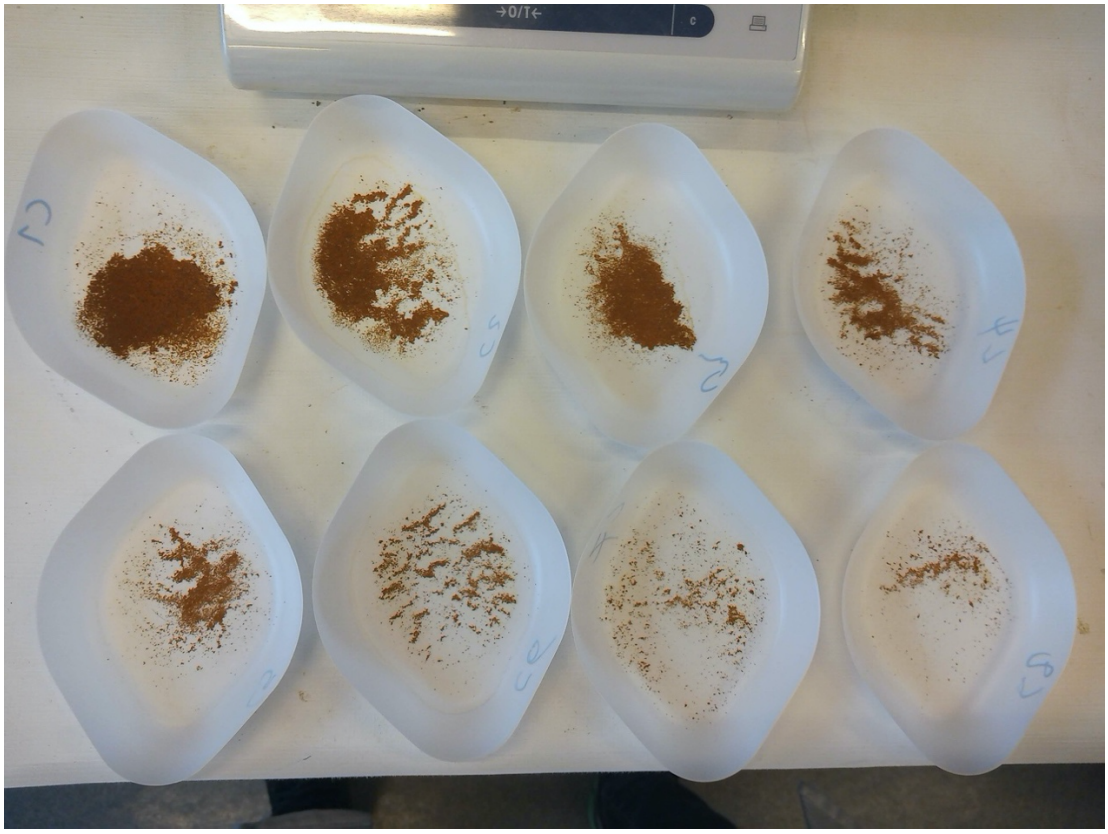

Figure 20 – Collected magnetic content of model drilling fluid after eight magnetic extraction

4.2 Field Drilling Fluid Samples

The number of 47 drilling fluid samples were collected from a multilateral production well drilled with the semi-submersible drilling rig located in one of the North sea's fields. For better understanding, we call this well A. The drilling operation started in late April 2020 and ended in May 2020. This rig was equipped with conventional ditch magnets that were formed with five vertical rod magnets to remove magnetic debris. To know more about the different types of ditch magnets, refer to (Strømø 2016). The rod magnets were mounted on a plate that was placed on the base of the flowline. The magnets were covered with filter bags which was part of the design to make the cleaning of the magnets easier and faster. When the drilling fluid goes through the flowline, the steel particles of the drilling fluid get attached to the filter bags instead of the magnets when they reach the near vicinity of the ditch magnets. This bag helps to avoid direct contact between the magnetic particles and the magnetic rods. This type of ditch magnet system is shown in Figure 21.

Figure 21 – Ditch magnet system (Strømø 2016)

The first and the last drilling fluid sample were collected on 29.04.2020 and 19.05.2020 in order. All the drilling fluid samples were brought to the University of Stavanger and tested with the developed measurement system described in the methodology section. The samples were mixed for five minutes, and 500 ml of the samples were poured into the beaker for testing. For instance, Figure 22 shows the weight of magnetic content collected after performing eight magnetic extractions on the WBM17 drilling fluid sample. Here, the same trend as model drilling fluid can be seen. But the curve becomes horizontal after performing several magnetic extractions. This observation which was almost the same for all the drilling fluid samples, is interesting. Because it might indicate if we continue the extraction process after the eighth magnetic extraction, we only collect non-magnetic particles, and not much magnetic content is left in the drilling fluid.

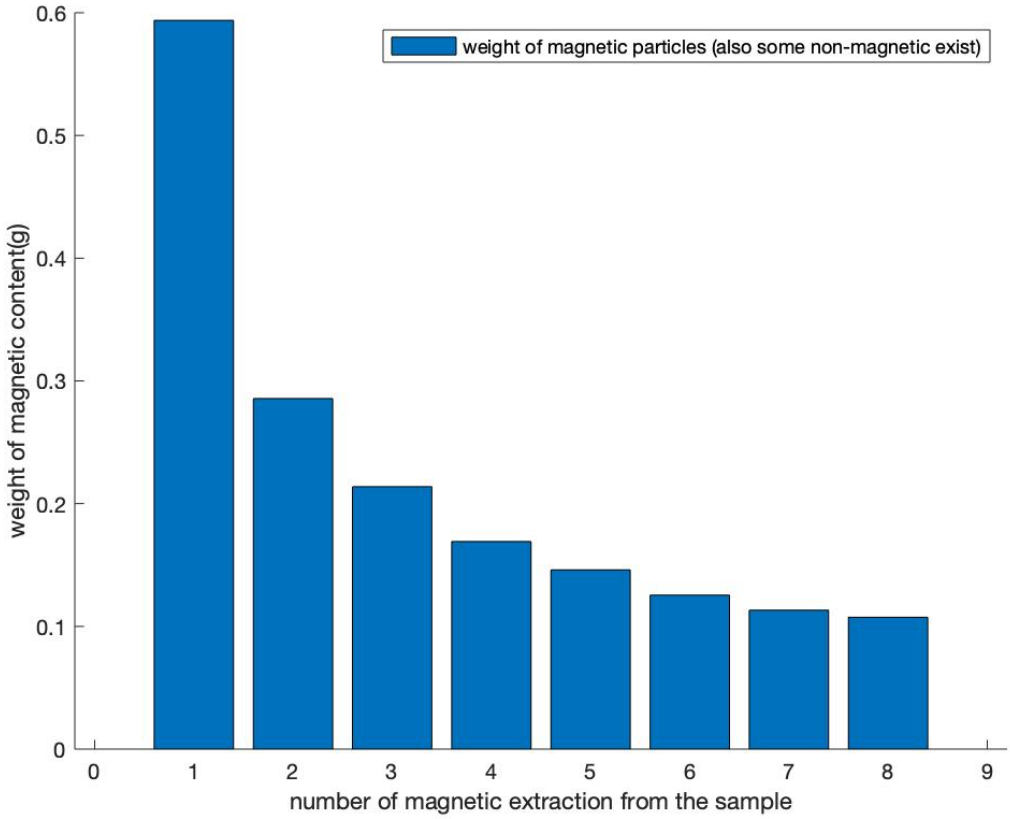

Figure 22 – Measured magnetic content of sample WBM 17 after eight magnetic extractions

Figure 23 shows the collected content in each magnetic extraction from the WBM17 drilling fluid sample and gives good information if compared to the measurement figure (Figure 22). If we take a closer look at the figure, we can see two different colors in the content, which might reveal the exitance of magnetic (dark color) and non-magnetic (brighter color) particles since the real drilling fluids also contain clay minerals, weight material particles and other types of material. Experience from other industries also can help us clarify this issue. Strong magnetic field and high-gradient magnetic field are used in the other fields to separate the particles with very low magnetic susceptibility by introducing ferromagnetic into the solution. There are two phenomena involved in this separation process: (a) the particles interact with each other, and flocculation occurs because of induced dipole-dipole interaction (b) weakly magnetic particles are filtered using the ferromagnetic particles. In the present experiment, when the magnet is immersed in the drilling fluid, forming a strong magnetic field, the non-magnetic or very weakly magnetic particles and ferromagnetic particles interact with each other and form flocs. Finally, these flocs are attracted by the magnet. This phenomenon makes the accurate measurement of net magnetic particles more challenging because the other

particles are also entrapped. Further in this work, a data-driven approach will be provided to find the net amount of magnetic content.

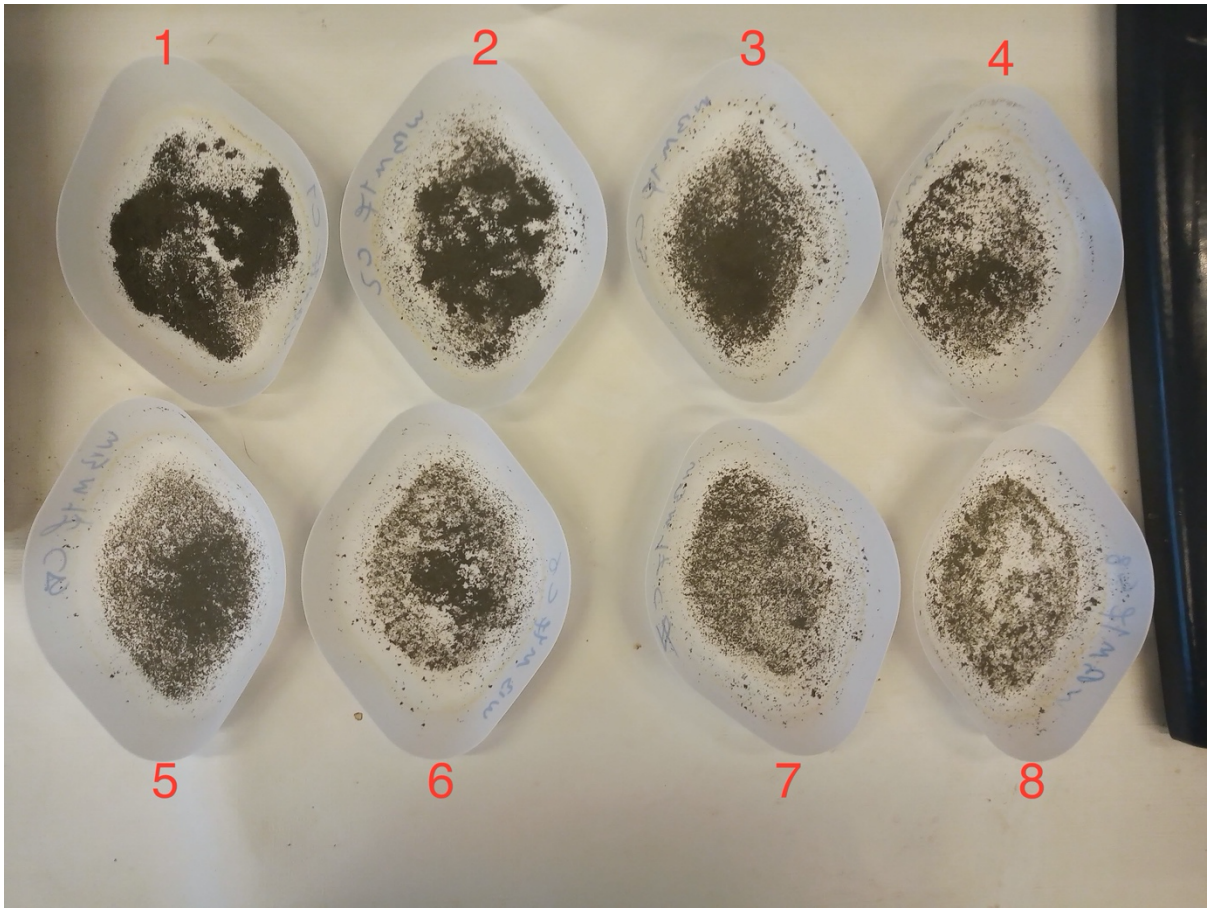

Figure 23 – Collected magnetic content of sample WBM 17

The date and time that the samples were collected on the rig site are provided in Table 7. Data about the measured weight of magnetic contamination of drilling fluid samples is in the same table.

Table 7 – Measurement data set of field drilling fluid samples

Sample number	Depth of the sample	Date of sample	Time of sample	Weight of magnetic content measured after each magnetic extraction from the sample(g)								Gross sum of the extracted magnetic content(g)
				1	2	3	4	5	6	7	8	
WBM4	7221m	16-May	15:30	0.3929	0.2419	0.1446	0.1268					0.9062
WBM5	-	03-May	21:15	0.329	0.204	0.1682	0.1454					0.8466
WBM6	8012m	18-May	15:10	0.676	0.2546	0.176	0.1234					1.23
WBM7	-	08-May	02:30	0.3214	0.1715	0.1534	0.1098					0.7561
WBM8	6387m	11-May	03:15	0.3025	0.1714	0.1028	0.0876	0.0756	0.0598	0.0664	0.0396	0.9057
WBM9	8103m	18-May	22:00	0.5492	0.2768	0.2122	0.1846					1.2228
WBM10	-	07-May	22:00	0.3585	0.2027	0.139	0.1196	0.1117	0.0924	0.0886	0.0731	1.1856
WBM12	7518m	17-May	10:00	0.4261	0.1914	0.1303	0.0924	0.0946	0.0883	0.0775	0.0815	1.1821
WBM13	-	07-May	17:30	0.3496	0.2197	0.1593	0.1407	0.1274	0.1132	0.0951	0.1178	1.3228
WBM14	6237m	10-May	21:20	0.3564	0.1349	0.0686	0.0565	0.0498	0.0337	0.0312	0.0246	0.7557
WBM15	5934m	09-May	21:25	0.4675	0.2501	0.1776	0.1523	0.1274	0.1124	0.1185	0.1023	1.5081
WBM16	5741,6m	09-May	10:05	0.3787	0.2205	0.1575	0.1482	0.121	0.122	0.1046	0.0977	1.3502
WBM17	6005m	10-May	03:20	0.5938	0.2857	0.2138	0.1692	0.1461	0.1255	0.1132	0.1074	1.7547
WBM18	6890m	16-May	03:00	0.327	0.1522	0.113	0.0973	0.0947	0.0765	0.0759	0.0701	1.0067
WBM19	-	08-May	09:15	0.3589	0.2184	0.1575	0.1225	0.1208	0.1001	0.1055	0.0899	1.2736
WBM20	6446m	11-May	09:15	0.3619	0.1467	0.1042	0.0837	0.0688	0.0659	0.0728	0.0603	0.9643
WBM21	-	06-May	02:40	0.232	0.1421	0.1088	0.0992	0.087	0.0744	0.0688	0.0653	0.8776
WBM22	-	05-May	21:15	0.2391	0.1413	0.1364	0.0918	0.0785	0.0762	0.0751	0.0654	0.9038
WBM23	8233m	19-May	02:55	1.0969	0.3031	0.2023	0.162	0.1368	0.1134	0.1045	0.0943	2.2133
WBM24	-	02-May	03:00	0.179	0.0907	0.0626	0.0593	0.0518	0.0437	0.0449	0.0404	0.5724
WBM25	-	04-May	03:00	0.1449	0.0885	0.0604	0.057	0.0657	0.0629	0.0518	0.0586	0.5898

WBM26	6728m	15-May	20:35	0.3672	0.1572	0.0982	0.074	0.089	0.0499	0.0589	0.0425	0.9369
WBM28	7687m	17-May	20:40	0.3076	0.0994	0.0641	0.0354	0.0433	0.0392	0.0318	0.0336	0.6544
WBM29	-	30-Apr	03:30	0.0251	0.0106	0.0073	0.006	0.0056	0.0051	0.0038	0.0044	0.0679
WBM30	-	05-May	15:15	0.1721	0.0904	0.0646	0.0537	0.0457	0.0402	0.0384	0.0325	0.5376
WBM31	-	30-Apr	15:00	0.0934	0.0489	0.0409	0.0289	0.03	0.0317	0.0191	0.0219	0.3148
WBM32	-	29-Apr	09:00	0.1493	0.0843	0.0671	0.0536	0.0451	0.0429	0.0321	0.0341	0.5085
WBM34	-	03-May	10:00	0.1408	0.0683	0.0548	0.0465	0.0408	0.038	0.0317	0.0306	0.4515
WBM35	6530m	11-May	15:00	0.3712	0.1307	0.0893	0.0691	0.0625	0.0467	0.0471	0.0389	0.8555
WBM36	7950m	18-May	11:00	1.0838	0.2965	0.1993	0.1304	0.1102	0.0965	0.0818	0.0851	2.0836
WBM37	7595m	17-May	14:45	0.283	0.1172	0.094	0.0439	0.054	0.04	0.0203	0.0248	0.6772
WBM39	7048m	16-May	09:00	0.3456	0.1369	0.0941	0.0775	0.0549	0.0407	0.0302	0.0457	0.8256
WBM40	-	07-May	02:30	0.3049	0.156	0.119	0.0913	0.0898	0.0817	0.0695	0.0694	0.9816
WBM41	7398m	17-May	02:55	0.3566	0.1256	0.0885	0.0752	0.0617	0.0478	0.0473	0.0504	0.8531
WBM42	-	29-May	09:30	0.1923	0.0874	0.0568	0.0616	0.051	0.0436	0.0402	0.0344	0.5673
WBM43	-	04-May	15:00	0.1372	0.0912	0.0712	0.0603	0.0477	0.0443	0.0387	0.0376	0.5282
WBM44	-	03-May	05:00	0.1692	0.0779	0.0612	0.0597	0.0495	0.0458	0.0436	0.0409	0.5478
WBM45	5814m	09-May	15:00	0.3773	0.1948	0.1515	0.124	0.1038	0.0891	0.0882	0.0719	1.2006
WBM46	-	29-Apr	19:45	0.1199	0.0644	0.043	0.0292	0.0269	0.0218	0.0238	0.0208	0.3498
WBM47	-	08-May	15:40	0.3024	0.1663	0.1225	0.0999	0.0805	0.0816	0.0831	0.0689	1.0052
WBM48	8288m	19-May	14:20	0.3888	0.1645	0.1192	0.0998	0.0841	0.0738	0.0707	0.0648	1.0657
WBM49	-	03-May	20:30	0.1927	0.0966	0.0879	0.0797	0.0668	0.0556	0.0576	0.0513	0.6882
WBM50	7831m	18-May	02:55	0.4253	0.1495	0.0973	0.0622	0.0582	0.0518	0.0438	0.0358	0.9239
WBM51	-	29-Apr	14:00	0.1277	0.0631	0.0512	0.0415	0.0357	0.0408	0.0353	0.0318	0.4271
WBM52	6049m	09-May	09:15	0.8485	0.2888	0.2013	0.1556	0.1309	0.1252	0.1051	0.0919	1.9473
WBM54	5654m	09-May	04:10	0.3188	0.1834	0.1438	0.1127	0.0915	0.0813	0.0797	0.0632	1.0744
WBM55	6192m	09-May	14:00	0.1824	0.1116	0.077	0.058	0.0475	0.0411	0.0365	0.0365	0.5906
WBM56	-	30-Apr	10:00	0.0576	0.0315	0.0259	0.0198	0.0139	0.0166	0.0138	0.0041	0.1832
WBM57	-	06-May	20:50	0.2689	0.1487	0.1108	0.0909	0.0806	0.0735	0.067	0.0582	0.8986

WBM60	-	05-May	02:22	0.167	0.0825	0.0698	0.0493	0.0428	0.0414	0.039	0.0367	0.5285
WBM61	-	01-May	04:15	0.1216	0.0622	0.0478	0.0486	0.0359	0.0307	0.0342	0.0235	0.4045
WBM62	-	01-May	20:45	0.1105	0.0532	0.031	0.0198	0.0286	0.022	0.0213	0.0257	0.3121

It was found that there is a connection between the viscosity of the drilling fluids and the weight of content collected in the eighth magnetic extraction from the samples. The viscosity of three samples with high collected mass and three with low collected mass were measured, as shown in Figure 24 and Table 8.WBM23, WBM29 and WBM56 samples had the lowest and WBM13,WBM52 and WBM61 samples had the highest weight of magnetic content measured in eighth magnetic extraction. The viscosity profile is relatively higher for the latter three samples compared to the former three samples. An explanation for this can be that the more viscous and thicker the drilling fluid, the more solid particles suspended in the fluid, and thus more solid particles (clay, weight material, etc.) are attached to the glass tube when it is immersed in the drilling fluid. All the samples were non-Newtonian shear-thinning fluid as it is expected for WBDF, and the Herschel-Bulkley model was used to fit the data points.

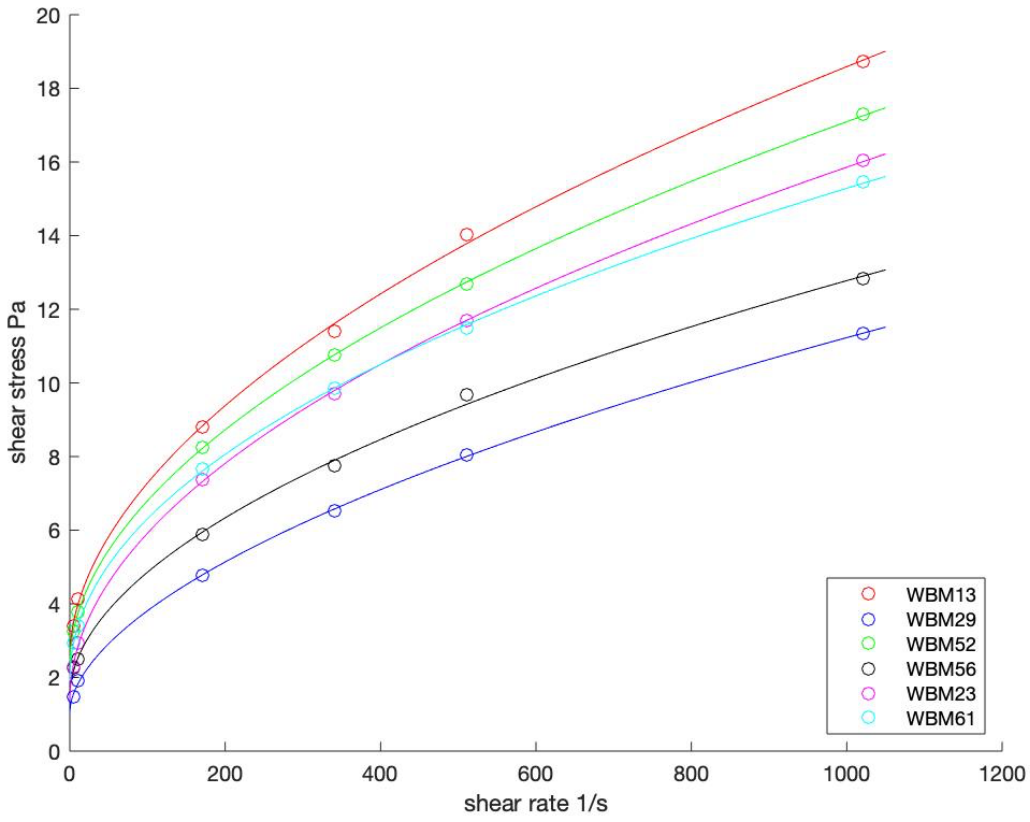

Figure 24 – Rheological behavior of samples with the highest and lowest weight of magnetic content measured in 8th magnetic extraction

Table 8 – Samples with the highest and lowest weight of magnetic content measured in 8th magnetic extraction

Sample number	WBM13	WBM23	WBM29	WBM52	WBM56	WBM61
Weight of magnetic content measured in 8th Magnetic extraction from the sample (g)	0.1178	0.0235	0.0044	0.0919	0.0041	0.0943

The last column of Table 7 represents the Gross Measured weight of magnetic contamination of the samples; it is equal to the sum of the magnetic content plus a small proportion of non-magnetic content collected from the sample after eight magnetic extractions (sum of eight side column).

Gross Measured weight of magnetic contamination of the samples ordered based on the date and time of the sampling are shown in Figure 25. WBM 23 sample has the highest amount of gross magnetic debris, which is 2.2133 g, and WBM 29 sample has the lowest, which is 0.0679 g. An average of 0.8807 g of gross magnetic material per 500 ml of the fluid samples was measured. From Figure 25, it is observed that the magnetic weight of the samples gradually increases as the drilling operation proceeds and the bit penetrates more into the formation. Notably, it can be seen that there are two peaks in the measurement of drilling fluid samples that were collected on 10th May and 18th May from the flowline. After 10th May, the magnetic content of drilling fluid samples decreased and became stable until 18th May when it increased again.

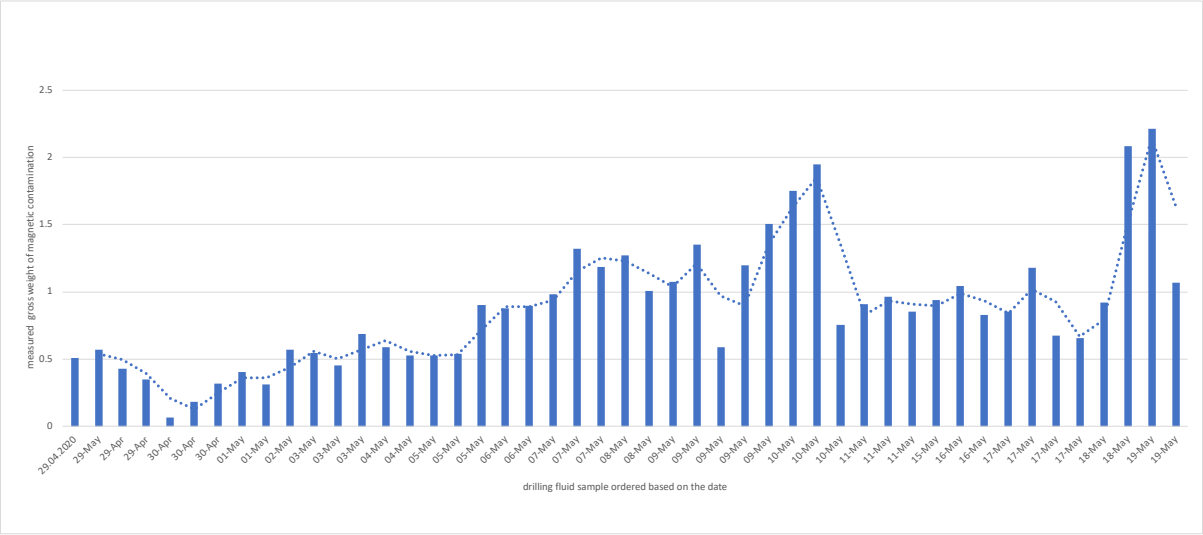

Figure 25 – The measured gross weight of magnetic contamination of drilling fluid samples ordered based on the date of sample

4.3 Finding the Net Amount of Magnetic Content of Drilling Fluid Samples

As it is described, non-magnetic or very weakly magnetic particles are also can be drawn to the strong magnet and make magnetic content measurement harder and thereby lower the accuracy of the magnetic content measurements. By analyzing the measurement data of sample WBM 17 from Figure 22 and, more generally, all of the samples, a solution is presented to find the net and pure amount of magnetic contamination in the sample. First, we determined an empirical correlation for measurement data of the WBM 17 sample:

$$W = AX^B + C$$

Where A, B, and C are determined from a fit of the above equation to data. W is the calculated weight of content collected after each magnetic extraction from the drilling fluid and X is the number of magnetic extractions. Figure 26 shows the measured weight after each magnetic extraction from the drilling fluid sample WBM17 (same as Figure 22) and the correlation that is fitted. As it was mentioned before, if we place the magnet inside the drilling fluid several times and get the same amount of content each time, we can say that not much magnetic content is left in the drilling fluid, and we only collect non-magnetic content. Using this concept and the obtained correlation, the number of magnetic extraction (n) in which the difference between the calculated weight of collected content of n and n-1 is less than 0.001 g is extrapolated:

$$W_n - W_{n-1} = (An^B + C) - (A(n-1)^B + C) < 0.001\ grams$$

The calculated weight at n ($W_n = An^B + C$) represents the weight of non-magnetic content collected at each magnetic extraction. Finally, to determine the net weight of the magnetic content of the sample, the weight of non-magnetic content is subtracted from measured weights at each magnetic extraction. Figure 26 demonstrates this procedure for the WBM17 sample.

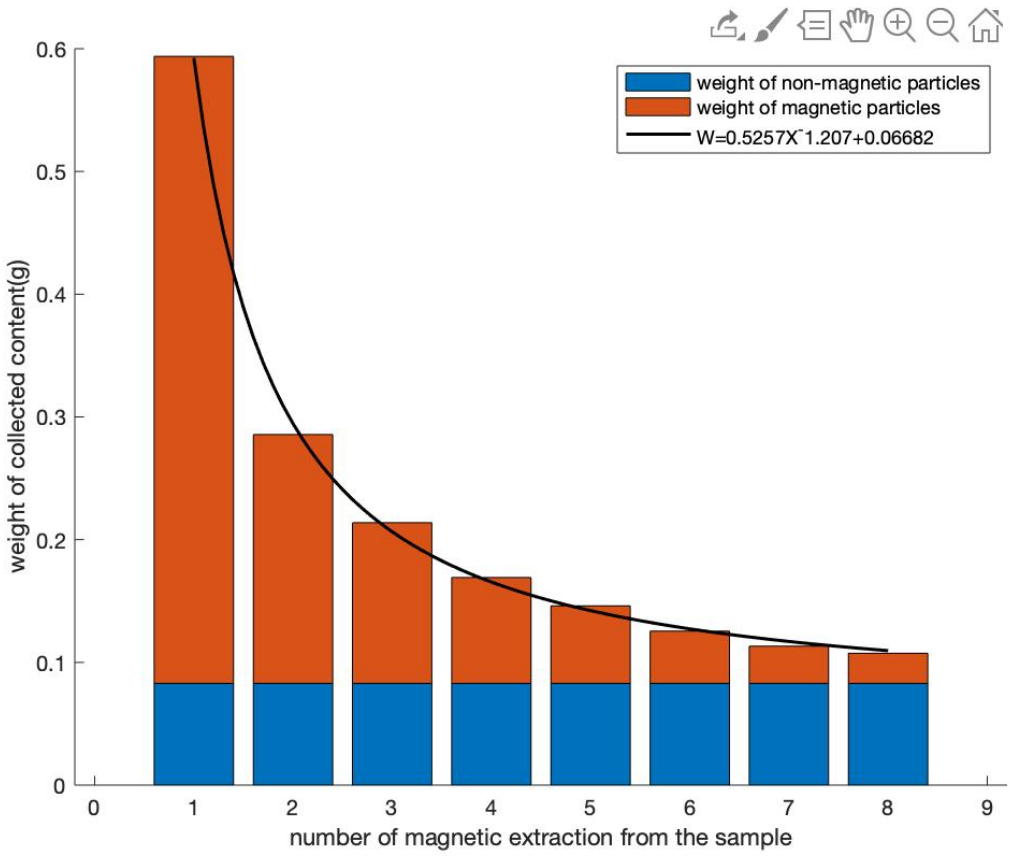

Figure 26 – The approach to find the net weight of magnetic content of sample WBM 17 (with extrapolation)

By doing the same procedure for all the samples, we can find the samples' net weight of magnetic contamination. Figure 27 shows these values for the drilling fluid samples ordered based on the date and time.

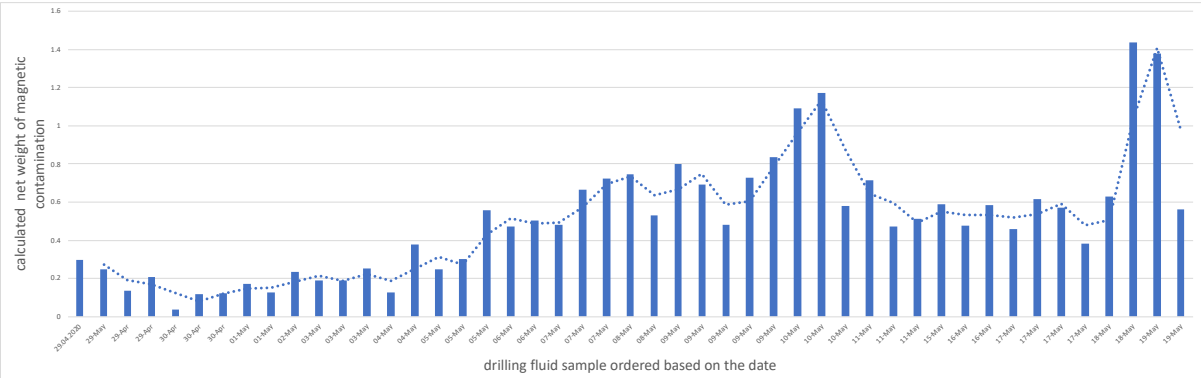

Figure 27 – Calculated net weight of magnetic contamination of drilling fluid samples ordered based on the date of the sample (with extrapolation)

WBM 36 sample had the highest amount of net magnetic debris, which was 1.4383 grams, and WBM 29 sample had the lowest, which was 0.0399 g. an average of 0.5075 g of

gross magnetic material per 500 ml of the fluid samples was collected. Therefore, the average net/gross ratio was $\frac{0.5075}{0.8807} = 0.5762$, which means that on average 57.6 % of the collected material from drilling fluid samples were magnetic.

Another approach to estimate the net weight of magnetic contamination of the samples without using extrapolation is also provided, which enables it to be applicable in the rig site. However, due to fluctuation in the measurement points, it is not recommended to use this approach, especially if the measured weight does not reach to constant level after eight times magnetic extraction. In this approach, we assume that the content that was collected in the eighth magnetic extraction was non-magnetic (Figure 28). Thereby, to determine the net weight of the magnetic content of the sample, the weight of non-magnetic content is subtracted from measured weights at each magnetic extraction. The estimated net weight of magnetic contamination of the samples with this approach is shown in Figure 29.

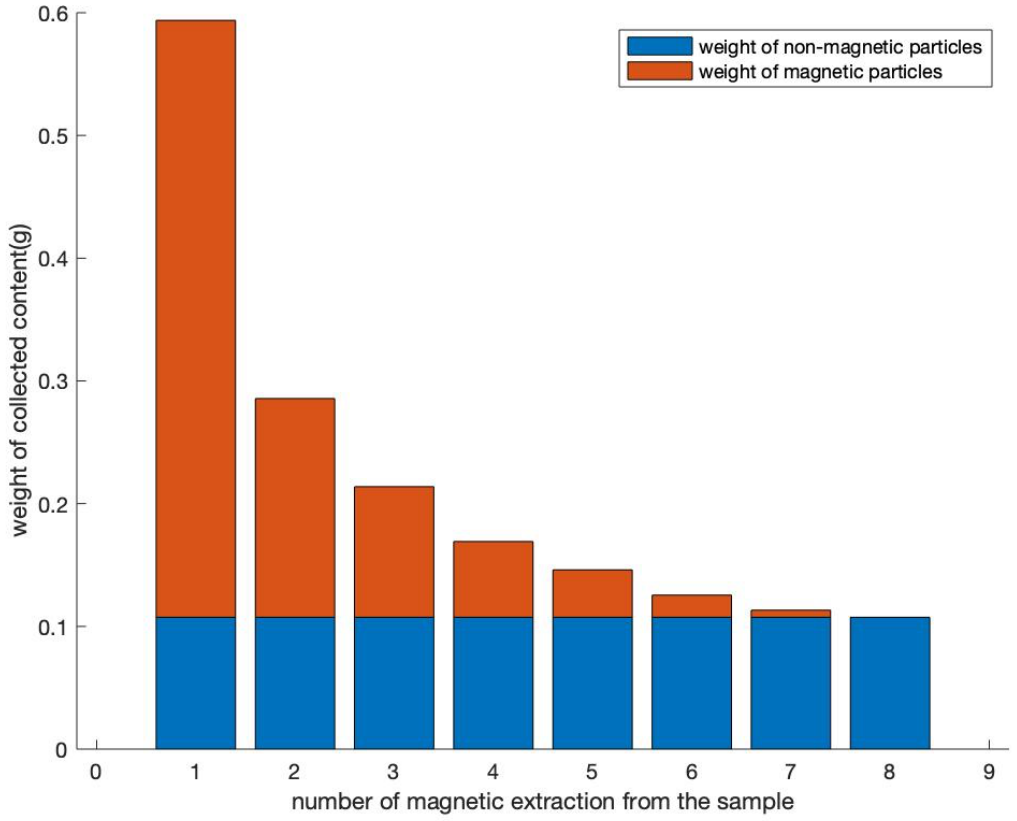

Figure 28 – The approach to find the net weight of magnetic content of sample WBM 17 (without extrapolation)

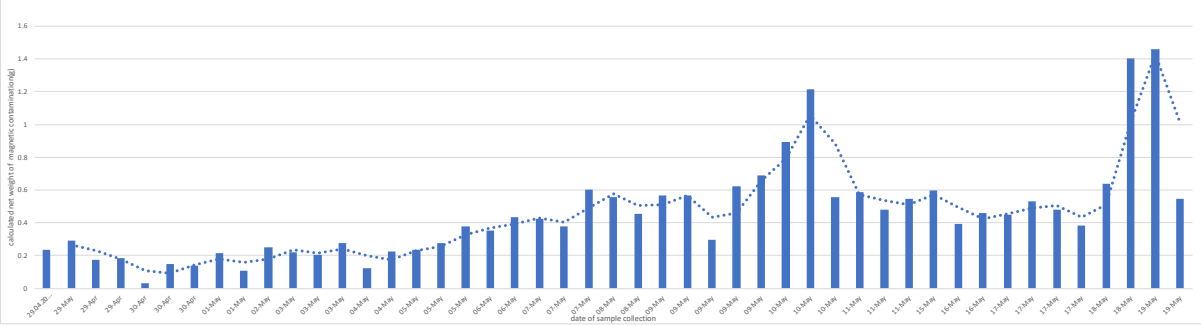

Figure 29 – Calculated net weight of magnetic contamination of drilling fluid samples ordered based on the date of samples (without extrapolation)

4.4 Microstructure Characterization

Scanning electron microscope (SEM) and Energy Dispersive X-ray Spectroscopy (EDS) test were performed on the sample WBM8 sample. As it can be seen from the magnified area in Figure 30 and EDS element analysis of spot three, which is provided in Table 9 white particles mostly represent iron. Other minerals such as quartz, barite, pyrite, mica, and bentonite also were detected in the specimen. The magnetic particles are in the scale micrometers. Consequently, it is believed that drilling fluid samples are collected after ditch magnets. The magnetic particles are expected to generate from metal abrasion and intensive contact since some of them had helical ridge.

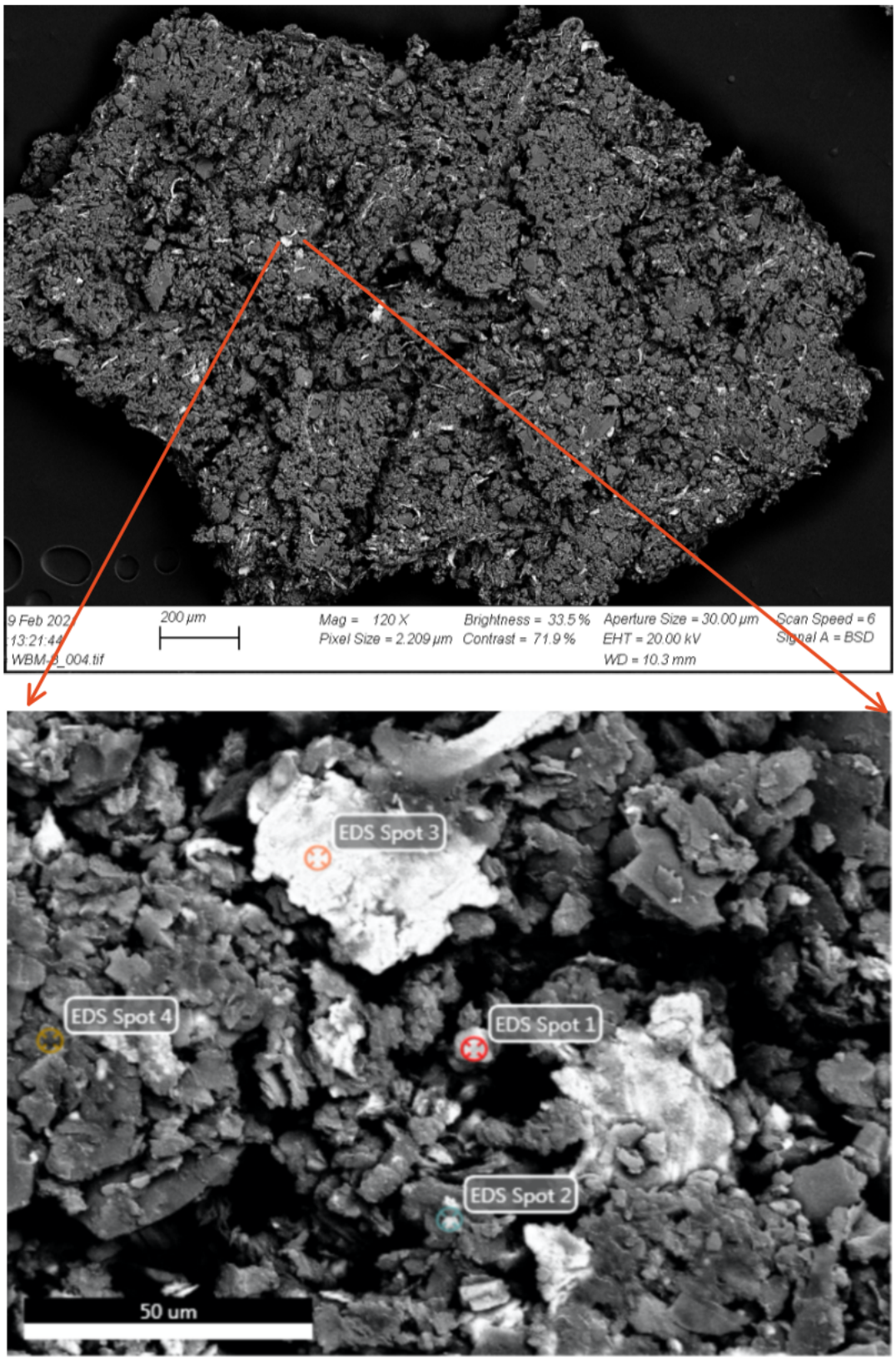

Figure 30 – Morphology of collected particles

Table 9 – EDS element analysis of spot 3

Element	Weight%	Atomic%	Net int.	Error%	Kratio	Z	A	F
C K	23.17	51.60	215.83	10.98	0.0610	1.1916	0.2317	1.0000
O K	5.72	9.56	148.57	10.62	0.0173	1.1452	0.2777	1.0000
Al K	7.41	7.35	388.29	7.97	0.0327	1.0259	0.4504	1.0018
Si K	1.44	1.38	91.34	11.58	0.0078	1.0495	0.5395	1.0029
Ca K	0.73	0.49	39.42	14.97	0.0069	0.9960	0.9516	1.0391
Cr K	4.79	2.46	193.81	4.65	0.0457	0.8963	0.9989	1.1188
Fe K	56.74	27.17	1613.32	2.03	0.4833	0.8924	0.9975	1.0041

The crystallography of the collected material by the magnet was investigated by an X-ray diffraction test. Quartz was the dominant detected crystal phase by phase-matching to a database that contains identified mineral structure, as shown in Figure 31. Iron was also detected in the X-ray pattern of collected material.

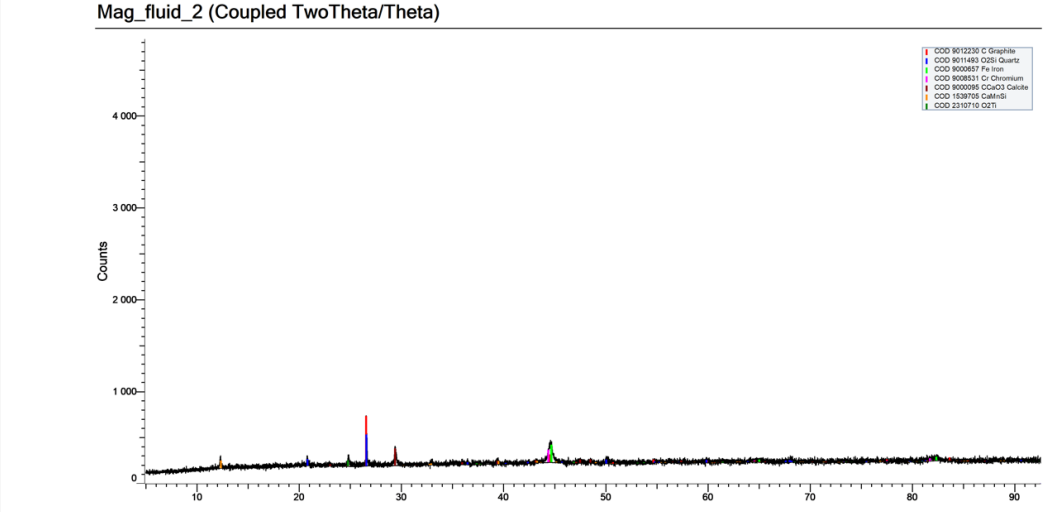

Figure 31 – XRD pattern of collected material

4.5 Ditch Magnet

The data of ditch magnets from the same well (well A) that the samples were collected are provided in Figure 32. The ditch magnets were cleaned every two or three hours by roughnecks, and the attached magnetic contamination to these magnets was measured. It should be noted that measured weights consist of drilling fluid filtrate and other solid particles that stick to the magnets in the flowline. Hence, the weights of magnetic contents attracted to the ditch magnets are lower than the values shown in Figure 32. The experience from another well that underwent milling operation reveals that about 45% of materials collected by ditch magnets were swarf. This can be a huge finding since it indicates a higher amount of metallic swarf in the well after milling, which can finally agglomerate on the downhole tools or end up on the shale shakers. In their measurements, they washed the collected material to find the dry swarf.

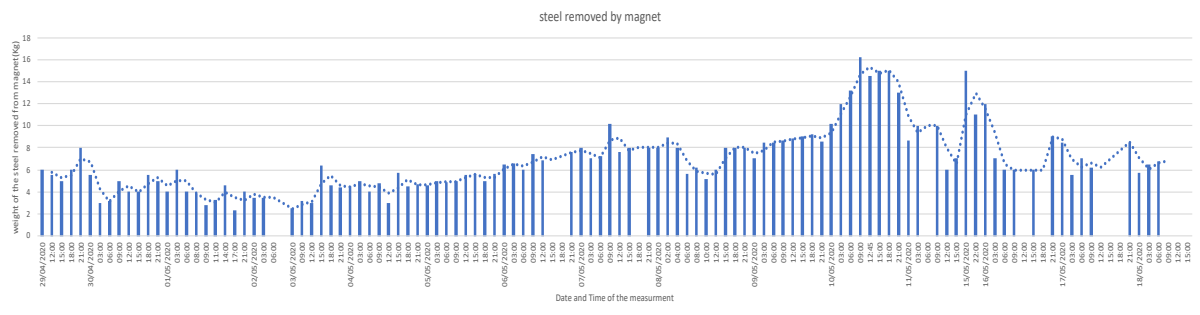

Figure 32 – Ditch magnet removed weights every 3 or 2 hours

Comparing measurement data of the drilling fluid samples in Figure 25 to ditch magnet data, it can be seen that both follow the same trend, and measured magnetic weights gradually increases with time. In both of the figures, an unusual increase in the measurements is observed on 10th April. This could be a sign of deficiency of the ditch magnet if the drilling fluid samples are collected from downstream of magnets since it has not been able to eliminate the magnetic content of the drilling fluid.

Common factors that can contribute to the production of magnetic debris were investigated. Inclination, the section of drilling, and the dogleg severity are known to be some of these factors. Dogleg severity is the parameter that shows how the trajectory of the well changes quickly. If the casing is cemented in those locations, there is excessive abrasion because of higher contact between the drillstring and the casing. If uncemented, there is also

friction between the drillstring and the formation, which at the end can result in magnetic contamination. Figure 33 demonstrates the dogleg severity of the well as a function of the date of the drilling operation.

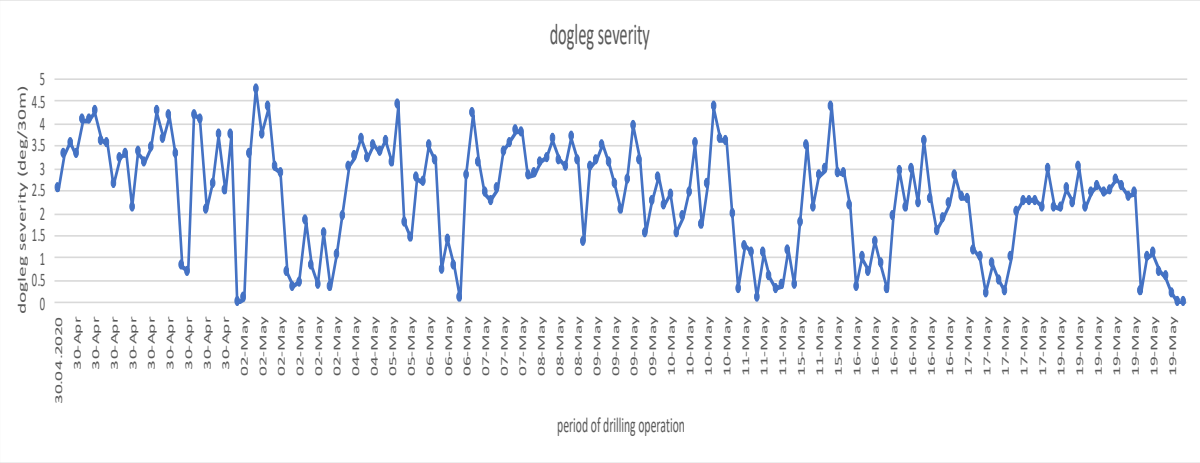

Figure 33 – Dogleg severity of the well

Any anticipated relation between the dogleg severity and magnetic contamination removed by this specific type of conventional ditch magnet could not be seen by comparing Figure 32 and Figure 33.

4.6 Comparing the before and after ditch magnet samples

Six double set samples were collected from another well (well B) that was drilled with a semi-submersible rig in one of the North Sea fields. These double set samples were collected from the flowline at the same time, one before and one after the ditch magnet. This well was equipped with flow positioned ditch magnet. Weight of the magnetic content of these samples was measured with the established procedure. Figure 34, Figure ***35***, Figure ***36***,Figure ***37***,Figure ***38*** , and Figure ***39*** show the measured magnetic content of the before and after ditch magnet drilling fluid samples.

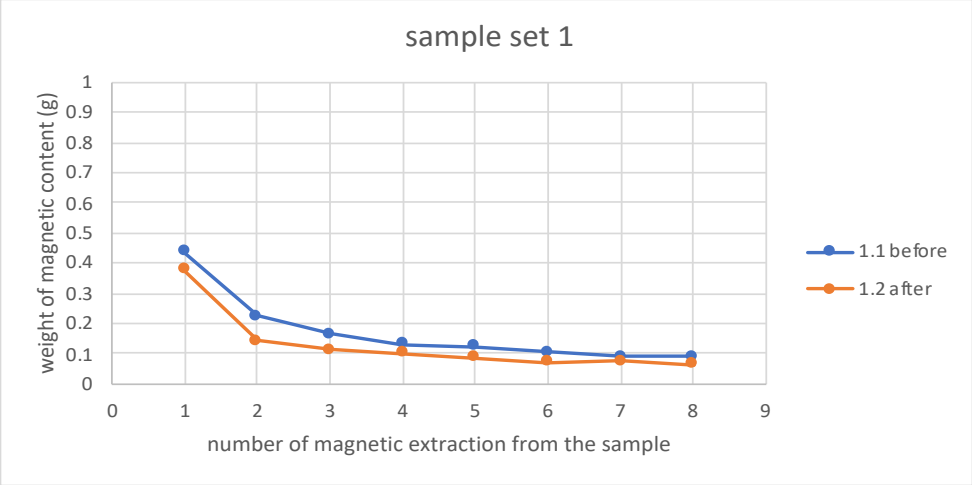

Figure 34 – Measured magnetic content of sample set 1 after eight magnetic extractions

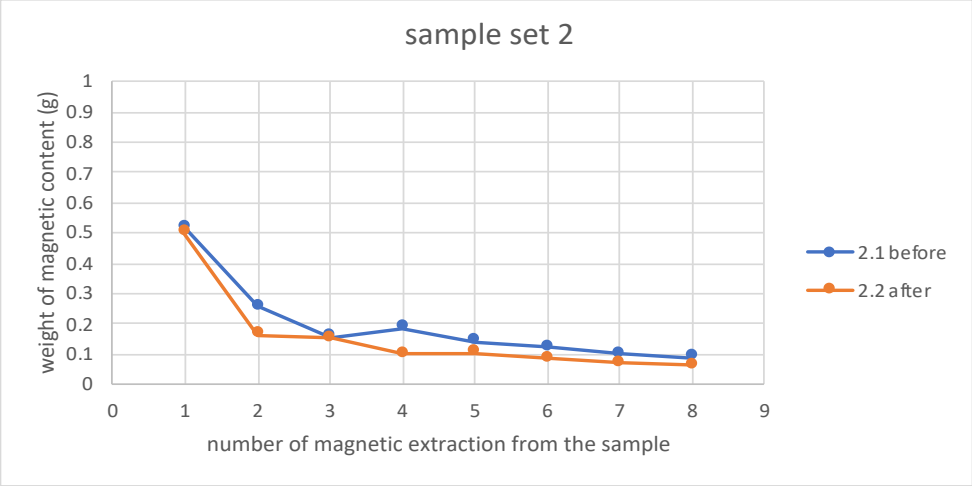

Figure 35 – Measured magnetic content of sample set 2 after eight magnetic extractions

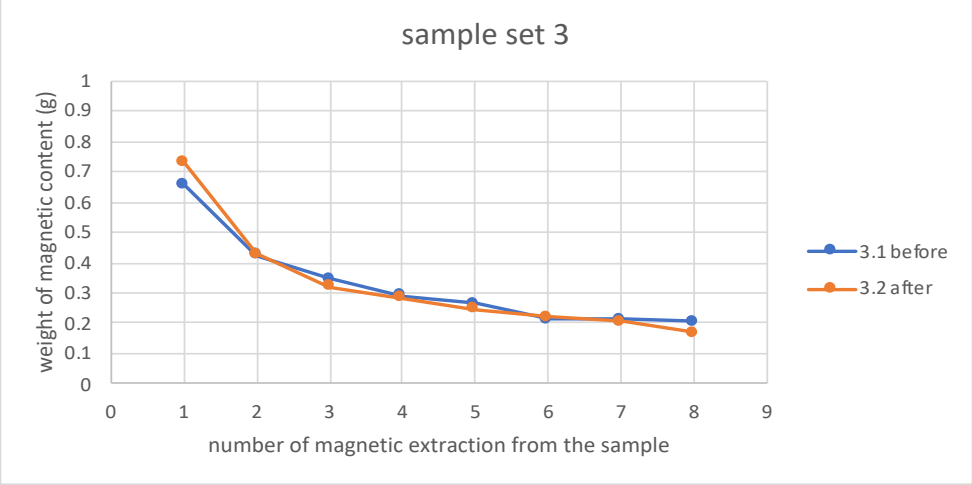

Figure 36 – Measured magnetic content of sample set 3 after eight magnetic extractions

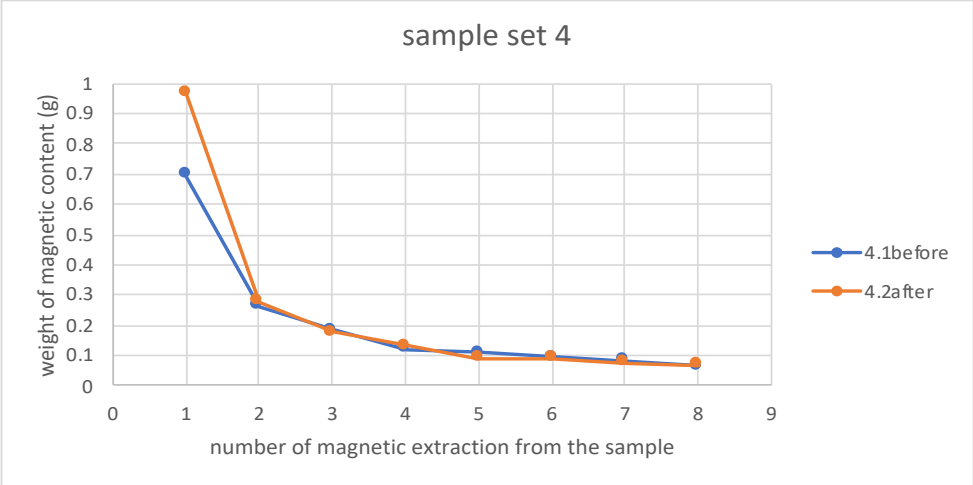

Figure 37 – Measured magnetic content of sample set 4 after eight magnetic extractions

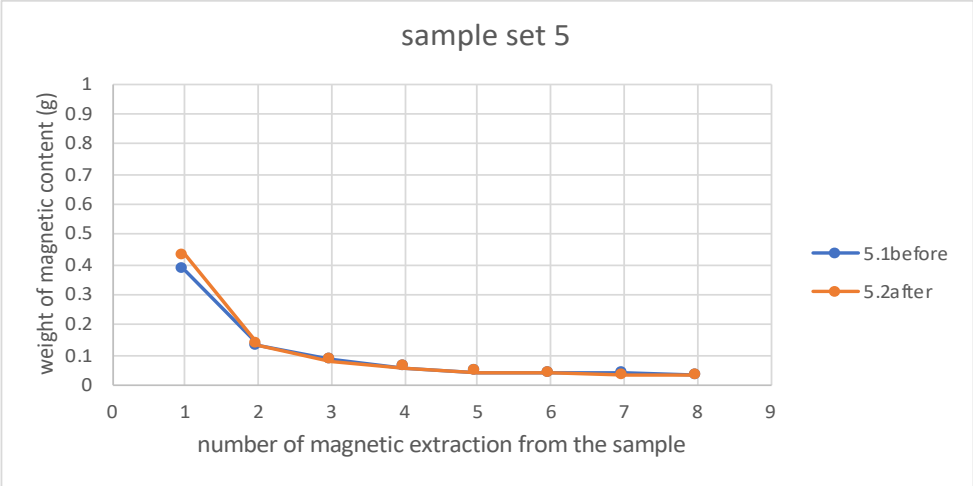

Figure 38 – Measured magnetic content of sample set 5 after eight magnetic extractions

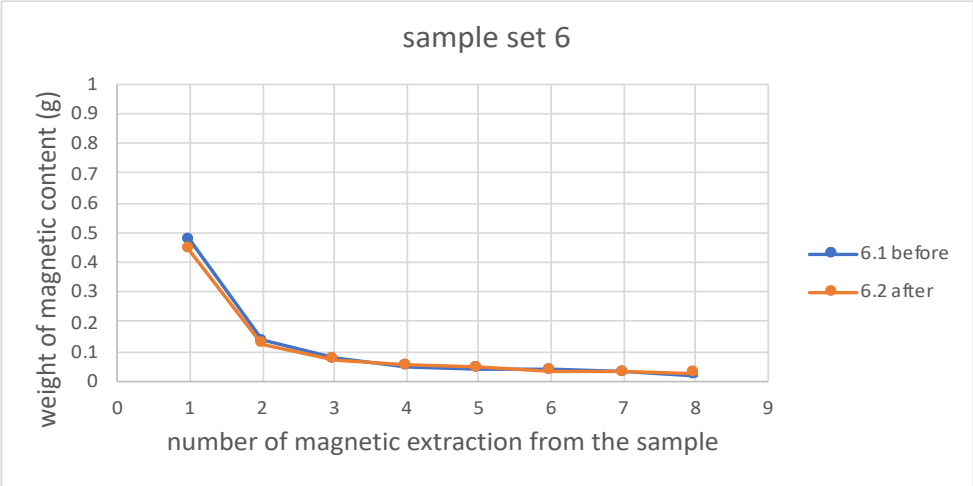

Figure 39 – Measured magnetic content of sample set 6 after eight magnetic extractions

All the samples except sample set 3 reached a plateau with a small amount of magnetic content extracted in the eighth magnetic extraction. In the daily report of the well, it was reported that at the time of collecting sample set 3 substantial amounts of black sticky substance was observed on the ditch magnets. This could explain the complexity of measuring the magnetic content of sample set 3. Comparing the weight of magnetic content extracted from the sample set 3 and 4, it can be noted that in the first magnetic extraction, higher weight of magnetic content was extracted from the sample set 4. However, in the eighth magnetic extraction higher weight of magnetic content was extracted from sample set 3. Given the fact that bigger particles are normally collected in the first extraction, sample set 4 contained coarser magnetic particles. A considerable amount of magnetic content that was removed from the ditch magnet at the time of collecting sample set 4 (Table 10) also can justify this since ditch magnets normally remove the bigger magnetic particles. By comparing the weight of magnetic contamination of the samples collected from upstream and downstream of this type of ditch magnet, no helpful difference was observed that could assist in evaluating the performance of the ditch magnet. Additionally, uncertainties in sampling the drilling fluids, such as the location of the samples and mistakes in labeling, could make the interpretation of the results harder.

Table 10 – Data of measured magnetic content of the sample sets and the ditch magnets

Number of sample set	Date of the sample	Time of the samples	Magnetic content removed from ditch on that time (Kg)	Gross sum of magnetic content (g) extracted after eight magnetic extractions	
				Before the ditch magnet	After the ditch magnet
1	25/03/2021	11:15	12	1.3696	1.027
2	26/03/2021	15:10	9	1.5704	1.2404
3	27/03/2021	10:20	10.5	2.6098 (3.7147)[1]	2.6006
4	29/03/2021	09:40	17.5	1.6173	1.8788
5	02/04/2021	14:40	NA	0.7999	0.8432
6	03/04/2021	14:10	10	0.8697	0.8343

[1] Gross sum of extracted magnetic content (g) after 16 magnetic extractions

Figure 40 shows the measured magnetic contamination of the samples and the magnetic contamination that was removed from the magnet at the time of sampling. Unlike well A (investigated earlier), an obvious relationship between the measured magnetic content of the samples and the ditch magnet measurement could not be observed.

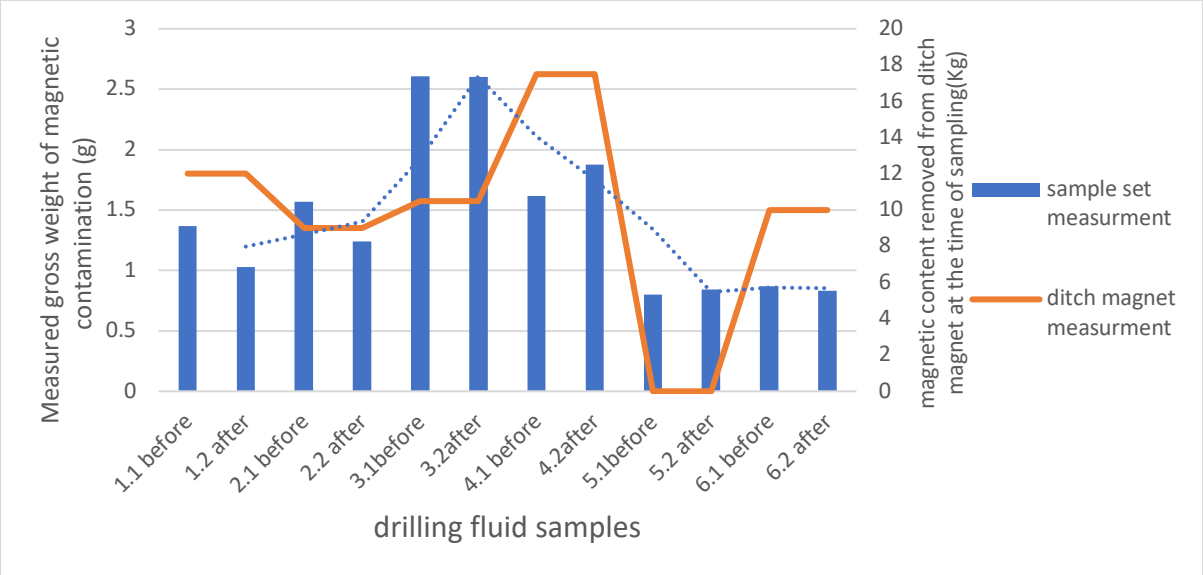

Figure 40 – Measured magnetic content of sample set compared to ditch magnet removed weight

5 Conclusion

A measurement procedure was developed to measure the weight of magnetic contamination of the drilling fluid, which can compensate for the lack of an established standard for measurement. Using this method, the weight of magnetic contents of 48 water-based drilling fluid samples was measured. This method was found to have a reasonable quality in presenting the magnetic content of a drilling fluid sample. Measuring the magnetic contamination of drilling fluid helps to inspect the performance of mounted ditch magnets in offshore rigs and whether the cleaning routine of the magnets is proper enough or not.

SEM analysis reveals that collected particles by the magnet can also be non-magnetic or weakly magnetic and be attracted to the magnet as a result of being attached to a flocculated structure of magnetic particles. Considering the fact that the non-magnetic particles can also take part in measurements, finding the net weight of magnetic contamination of drilling fluid is not straightforward with simple drilling fluid laboratory equipment. It was found that there is a correlation between the mass of gross collected magnetic content from drilling fluid samples and the repetition of magnetic extraction. The weight of gross collected magnetic content becomes constant after several times immersing the magnet inside the drilling fluid, which is a sign of not many magnetic particles left in the drilling fluid. In this manner, an approach was provided to find the net amount of magnetic content.

No meaningful difference was observed when the weight of magnetic content of samples collected from downstream and upstream of the ditch magnet compared to each other. Consequently, evaluating the performance of the ditch magnet in this way was not possible.

6 References

Akasofu, Syun-Ichi, and Louis J. Lanzerotti. 1975. “The Earth’s Magnetosphere.” *Physics Today* 28(12):28–35. doi: 10.1063/1.3069238.

American Petroleum Institute. 2014. *Recommended Practice for Testing Oil-Based Drilling Fluids*. API Recommended Practice 13B2. Washington, DC, USA: API.

Amundsen, Per A., Songxiong Ding, Biplab K. Datta, Torgeir Torkildsen, and Arild Saasen. 2010. “Magnetic Shielding During MWD Azimuth Measurements and Wellbore Positioning.” *SPE Drilling & Completion* 25(02):219–22. doi: 10.2118/113206-PA.

Amundsen, Per A., Torgeir Torkildsen, and Arild Saasen. 2006. “Shielding of Directional Magnetic Sensor Readings in a Measurement While Drilling Tool for Oil Well Positioning.” *Journal of Energy Resources Technology* 128(4):343–45. doi: 10.1115/1.2358151.

Bakker, Chris J. G., and Remmert de Roos. 2006. “Concerning the Preparation and Use of Substances with a Magnetic Susceptibility Equal to the Magnetic Susceptibility of Air.” *Magnetic Resonance in Medicine* 56(5):1107–13. doi: 10.1002/mrm.21069.

Bang, Jon, Torgeir Torkildsen, Bjoern T. Bruun, and Stein Tjelta Havardstein. 2009. “Targeting Challenges in Northern Areas Due to Degradation of Wellbore Positioning Accuracy.” in *SPE/IADC Drilling Conference and Exhibition*. Amsterdam, The Netherlands: Society of Petroleum Engineers.

Brooks, A. G., P. A. Gurden, and K. A. Noy. 1998. “Practical Application of a Multiple-Survey Magnetic Correction Algorithm.” in *SPE Annual Technical Conference and Exhibition*. New Orleans, Louisiana: Society of Petroleum Engineers.

Buchanan, Andrew, Carol Finn, Jeffrey J. Love, E. William Worthington, Fraser Lawson, Stefan Maus, Shola Okewunmi, and Benny Poedjono. 2013. “Geomagnetic Referencing--the Real-Time Compass for Directional Drillers.” *Oilfield Review* 25(3):32–47.

Cullity, B. D., and C. D. Graham. 2009. *Introduction to Magnetic Materials*. 2nd ed. Hoboken, N.J: IEEE/Wiley.

Ding, S., B. K. Datta, A. Saasen, and P. A. Amundsen. 2010. “Experimental Investigation of the Magnetic Shielding Effect of Mineral Powders in a Drilling Fluid.” *Particulate Science and Technology* 28(1):86–94. doi: 10.1080/02726350903500781.

Eastman, H. John. 1937. “The Art of Oil Well Surveying and Controlled Directional Drilling.”

Edvardsen. 2016. “Effects of Geomagnetic Disturbances on Offshore Magnetic Directional Wellbore Positioning in the Northern Auroral Zone.” PhD thesis, Universitet i Tromso, Tromso,Norway.

Edvardsen, I. .., T. L. Hansen, M. .. Gjertsen, and H. .. Wilson. 2013. “Improving the Accuracy of Directional Wellbore Surveying in the Norwegian Sea.” *SPE Drilling & Completion* 28(02):158–67. doi: 10.2118/159679-PA.

Edvardsen, Inge, Erik Nyrnes, Magnar G. Johnsen, Truls L. Hansen, and Ingelinn Aarnes. 2019. “How To Manage Geomagnetic-Field Disturbances in the Northern Auroral Zone To Improve the Accuracy of Magnetic Measurement-While-Drilling Directional Surveys.” *SPE Drilling & Completion* 34(02):159–72. doi: 10.2118/189668-PA.

Fraden, Jacob. 2010. *Handbook of Modern Sensors: Physics, Designs, and Applications*. 4th ed. New York: Springer.

Garza, Travis, James Wimberg, Trevor Woolridge, Ezra North, and Keith Beattie. 2010. “Gyro Guidance Techniques and Telemetry Methods Prove Economical in Onshore Multi-Well Pad Drilling Operations in the Piceance Basin.”

Ge, Wei, Armando Encinas, Elsie Araujo, and Shaoxian Song. 2017. “Magnetic Matrices Used in High Gradient Magnetic Separation (HGMS): A Review.” *Results in Physics* 7:4278–86. doi: 10.1016/j.rinp.2017.10.055.

Getzlaff, Mathias. 2008. *Fundamentals of Magnetism*. Berlin ; New York: Springer.

Giorgio Pattarini. 2015. “Some Models for the Magnetization of the Drilling Mud.” Universitet i Stavanger, Norway.

Gooneratne, Chinthaka, Bodong Li, and Timothy Moellendick. 2017. “Downhole Applications of Magnetic Sensors.” *Sensors* 17(10):2384. doi: 10.3390/s17102384.

Gooneratne, Chinthaka P., Bodong Li, Max Deffenbaugh, and Timothy Moellendick. 2019. “Instruments for Well Navigation and Drilling Optimization Evaluation.” Pp. 47–61 in *Instruments, Measurement Principles and Communication Technologies for Downhole Drilling Environments*, edited by C. P. Gooneratne, B. Li, M. Deffenbaugh, and T. Moellendick. Cham: Springer International Publishing.

Griswold, E. H. 1929. “Acid Bottle Method of Subsurface Well Survey and Its Application.” *Transactions of the AIME* 82(01):41–49. doi: 10.2118/929041-G.

Hughes, James D. 1935. “Value of Oil-Well Surveying and Applications of Controlled Directional Drilling.”

Inglis, T. A. 1987. *Directional Drilling*. London ; Boston: Graham & Trotman.

International Organization for Standardization: Petroleum and Natural Gas Industries. 2008. *Field Testing of Drilling Fluids*. Report ISO 10414-1. Geneva, Switzerland: ISO.

ISCWSA. 2012. *Introduction to Wellbore Positioning*. University of the Highlands & Islands.

J. C. Maxwell Garnett. 1904. “XII. Colours in Metal Glasses and in Metallic Films.” *Philosophical Transactions of the Royal Society of London. Series A, Containing Papers of a Mathematical or Physical Character* 203(359–371):385–420. doi: 10.1098/rsta.1904.0024.

Kabirzadeh, Hojjat, Elena Rangelova, Gyoo Ho Lee, Jaehoon Jeong, Ik Woo, Yu Zhang, and Jeong Woo Kim. 2018. "Dynamic Error Analysis of Measurement While Drilling Using Variable Geomagnetic In-Field Referencing." *SPE Journal* 23(06):2327–38. doi: 10.2118/188653-PA.

Kuchel, P. W., B. E. Chapman, W. A. Bubb, P. E. Hansen, C. J. Durrant, and M. P. Hertzberg. 2003. "Magnetic Susceptibility: Solutions, Emulsions, and Cells." *Concepts in Magnetic Resonance* 18A(1):56–71. doi: 10.1002/cmr.a.10066.

Lowdon, R. M., and C. R. Chia. 2003. "Multistation Analysis and Geomagnetic Referencing Significantly Improve Magnetic Survey Results." in *SPE/IADC Drilling Conference*. Amsterdam, Netherlands: Society of Petroleum Engineers.

Mahmoud Khalifeh. 2016. "Materials for Optimized P&A Performance." University of Stavanger.

Marcon and Ostanina. 2012. "Overview of Methods for Magnetic Susceptibility Measurement." Kuala Lumpur, MALAYSIA.

Patel, Jignesh P., and Parsotam H. Parsania. 2018. "Characterization, Testing, and Reinforcing Materials of Biodegradable Composites." Pp. 55–79 in *Biodegradable and Biocompatible Polymer Composites*. Elsevier.

Pattarini, Giorgio, Kjartan Moe Strømø, Arild Saasen, Per Amund Amundsen, Jan Egil Pallin, and Helge Hodne. 2017. "Ditch Magnet Removal of Steel Particles." P. D011S007R004 in *Day 1 Wed, April 05, 2017*. Bergen, Norway: SPE.

Poedjono, Benny, Essam Adly, Mike Terpening, and Xiong Li. 2010. "Geomagnetic Referencing Service - A Viable Alternative for Accurate Wellbore Surveying." P. SPE-127753-MS in *All Days*. New Orleans, Louisiana, USA: SPE.

Poedjono, Benny, Diana Montenegro, Pete Clark, Shola Okewunmi, Stefan Maus, and Xiong Li. 2012. "Successful Application of Geomagnetic Referencing for Accurate Wellbore Positioning in a Deepwater Project Offshore Brazil." P. SPE-150107-MS in *All Days*. San Diego, California, USA: SPE.

Saasen, A., H. Hoset, E. J. Rostad, A. Fjogstad, O. Aunan, E. Westgård, and P. I. Norkyn. 2001. "Application of Ilmenite as Weight Material in Water Based and Oil Based Drilling Fluids." P. SPE-71401-MS in *All Days*. New Orleans, Louisiana: SPE.

Saasen, Arild, Songxiong Ding, Per Amund Amundsen, and Kristoffer Tellefsen. 2016. "The Shielding Effect of Drilling Fluids on Measurement While Drilling Tool Downhole Compasses—The Effect of Drilling Fluid Composition, Contaminants, and Rheology." *Journal of Energy Resources Technology* 138(5):052907. doi: 10.1115/1.4033304.

Saasen, Arild, Ole Henrik Jordal, David Burkhead, Per Cato Berg, Geir Løklingholm, Erik Sandtorv Pedersen, Jim Turner, and Michael J. Harris. 2002. "Drilling HT/HP Wells Using a Cesium Formate Based Drilling Fluid." P. SPE-74541-MS in *All Days*. Dallas, Texas: SPE.

Saasen, Arild, Jan Egil Pallin, Geir Olav Ånesbug, Alf Magne Lindgren, Gudmund Aaker, and Mads Rødsjø. 2019. “Removal of Magnetic Metallic Contamination – Improved Drilling Fluid Performance.” P. D031S012R002 in *Day 3 Thu, September 05, 2019*. Aberdeen, UK: SPE.

Saasen, Arild, Benny Poedjono, Geir Olav Ånesbug, and Nicholas Zachman. 2020. “Efficient Removal of Magnetic Contamination from Drilling Fluids - The Effect on Directional Drilling.” *Journal of Energy Resources Technology* 1–14. doi: 10.1115/1.4049290.

Shukla, Ashutosh Kumar, and Siavash Iravani, eds. 2019. *Green Synthesis, Characterization and Applications of Nanoparticles*. Amsterdam: Elsevier.

Spaldin, Nicola A. 2011. *Magnetic Materials: Fundamentals and Applications*. Cambridge; New York: Cambridge University Press.

Stefan Maus, Alexander Mitkus, Marc Willerth, and Andrew Reetz. 2017. *Challenges Related to Positional Uncertainty for Measurement While Drilling (MWD) in the Barents Sea*.

Strømø. 2016. “Ditch Magnet Performance.” Master’s thesis, University of Stavanger.

Strømø, Kjartan M., Arild Saasen, Helge Hodne, Jan Egil Pallin, and Gudmund Aaker. 2017. “Ditch Magnet Performance.” P. V008T11A057 in *Volume 8: Polar and Arctic Sciences and Technology; Petroleum Technology*. Trondheim, Norway: American Society of Mechanical Engineers.

Tarling, D. H., and F. Hrouda. 1993. *The Magnetic Anisotropy of Rocks*. 1st ed. London ; New York: Chapman & Hall.

Tellefsen, Kristoffer, Songxiong Ding, Arild Saasen, Per Amund Amundsen, Arild Fjogstad, and Torgeir Torkildsen. 2012. “The Effect of Drilling Fluid Content on Magnetic Shielding of Downhole Compasses in MWDs.” in *SPE Deepwater Drilling and Completions Conference*. Galveston, Texas, USA: Society of Petroleum Engineers.

Thorogood, John L., and David R. Knott. 1990. “Surveying Techniques With a Solid-State Magnetic Multishot Device.” *SPE Drilling Engineering* 5(03):209–14. doi: 10.2118/19030-PA.

Torkildsen, Torgeir, Inge Edvardsen, Arild Fjogstad, Arild Saasen, Per A. Amundsen, and Tor H. Omland. 2004. “Drilling Fluid Affects MWD Magnetic Azimuth and Wellbore Position.” in *IADC/SPE Drilling Conference*. Dallas, Texas: Society of Petroleum Engineers.

Torkildsen, Torgeir, Stein Tjelta Havardstein, John Lionel Weston, and Roger Ekseth. 2008. “Prediction of Wellbore Position Accuracy When Surveyed With Gyroscopic Tools.” *SPE Drilling & Completion* 23(01):5–12. doi: 10.2118/90408-PA.

Waag, Tor Inge, Torgeir Torkildsen, Per Amund Amundsen, Erik Nyrnes, and Arild Saasen. 2012. “The Design of BHA and the Placement of Magnetometer Sensors Influence How Magnetic Azimuth Is Distorted by the Magnetic Properties of Drilling Fluids.” *SPE Drilling & Completion* 27(03):392–405. doi: 10.2118/151039-PA.

Welker, Roger W. 2012. “Size Analysis and Identification of Particles.” Pp. 179–213 in *Developments in Surface Contamination and Cleaning*. Elsevier.

Wightman, W., Jalinoos, Frank, Hanna, Kanaan, and Sirles, Philip. 2004. *Application of Geophysical Methods to Highway Related Problems*. *Tech Report*. FHWA-IF-04-021. United States. Federal Highway Administration. Central Federal Lands Highway Division.

Williamson, H. S., P. A. Gurden, D. J. Kerridge, and G. Shiells. 1998. “Application of Interpolation In-Field Referencing to Remote Offshore Locations.” P. SPE-49061-MS in *All Days*. New Orleans, Louisiana: SPE.

Wilson, Harry, and Andrew G. Brooks. 2001. “Wellbore Position Errors Caused by Drilling Fluid Contamination.” in *SPE Annual Technical Conference and Exhibition*. New Orleans, Louisiana: Society of Petroleum Engineers.

Zawadzki, Jarosław, and Jan Bogacki. 2016. “Smart Magnetic Markers Use in Hydraulic Fracturing.” *Chemosphere* 162:23–30. doi: 10.1016/j.chemosphere.2016.07.058.

Appendix A

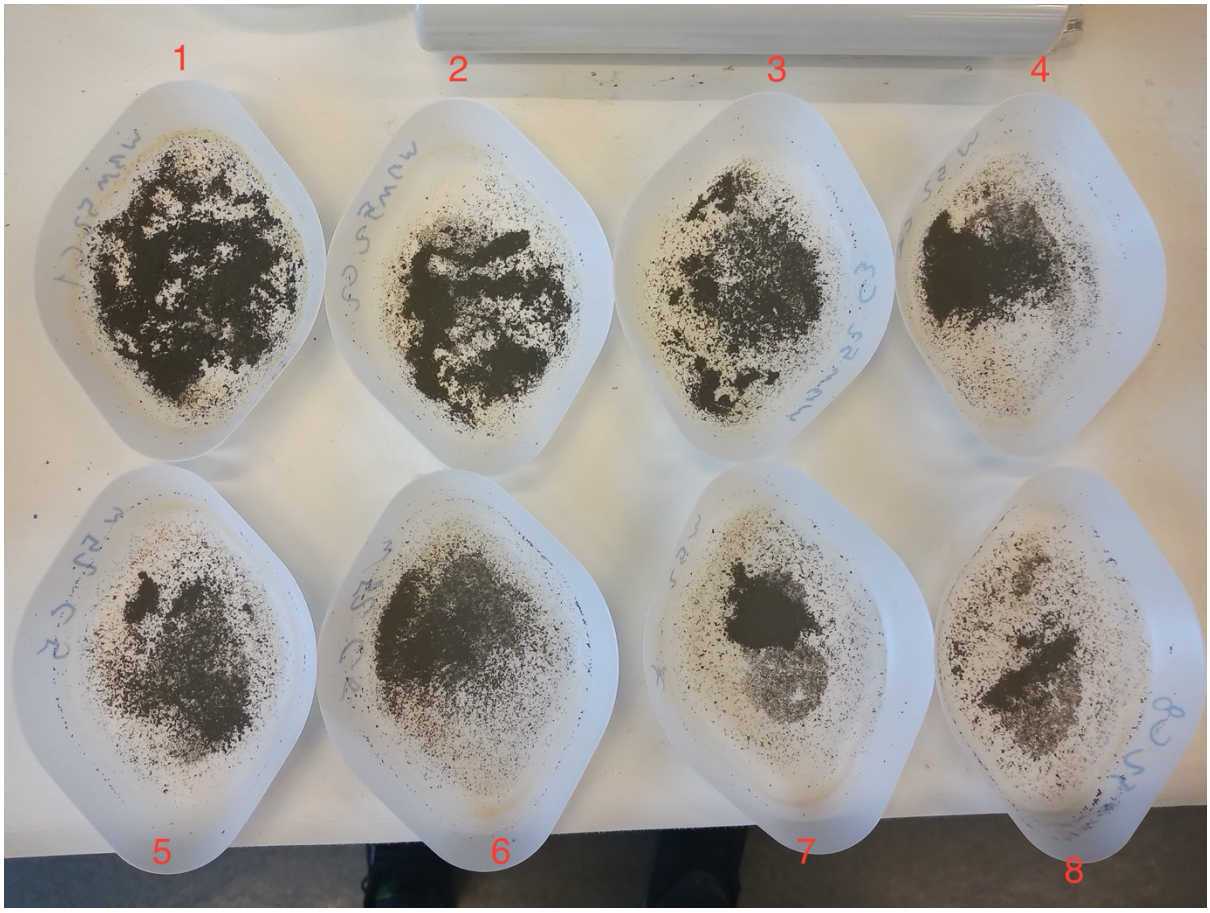

Figure 41 – Collected magnetic content of sample WBM 52 (high magnetic contamination)

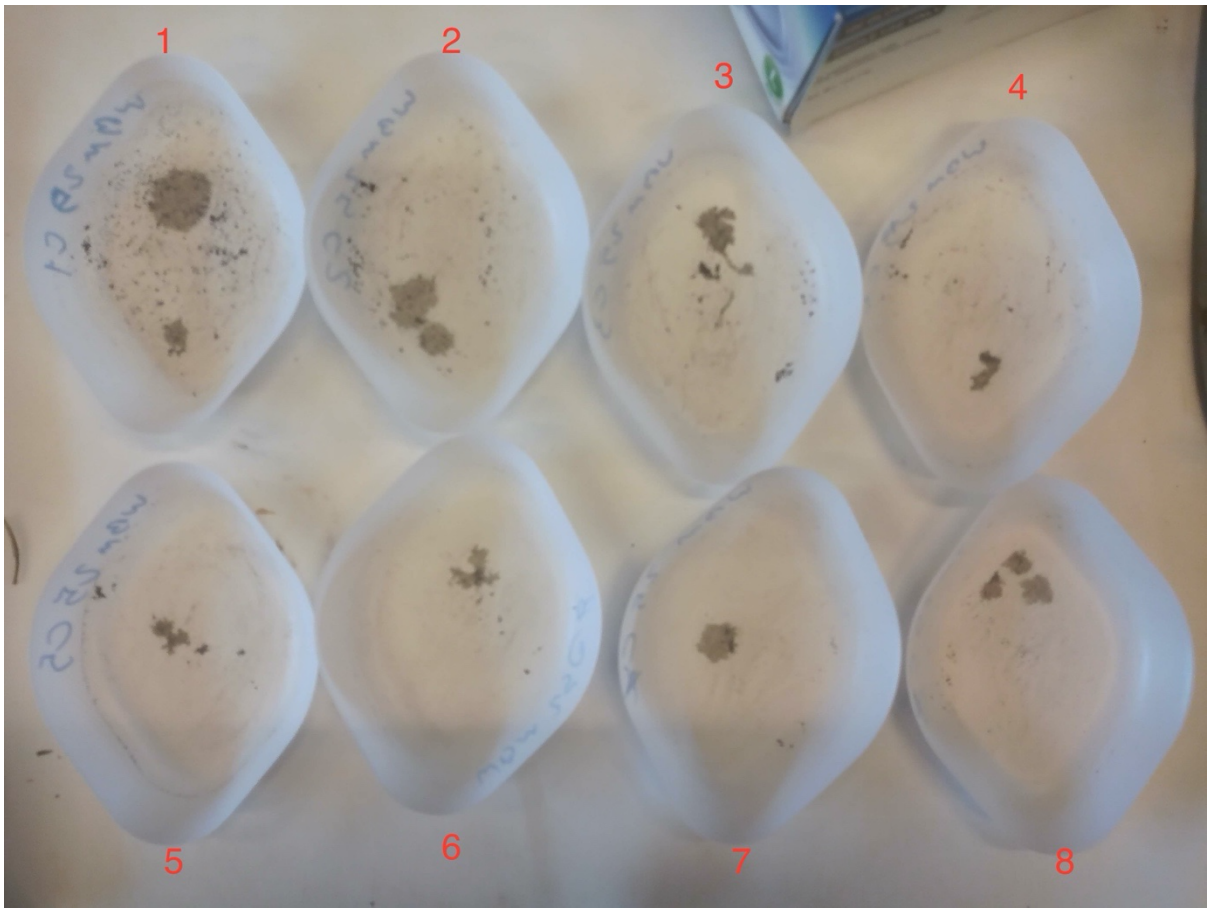

Figure 42 – Collected magnetic content of sample WBM 29 (low magnetic contamination)

Appendix B

SPE-207240-MS

Measuring and Analyzing the Magnetic Content of Drilling Fluid

Pouya Khalili, Arild Saasen, and Mahmoud Khalifeh, University of Stavanger; Bodil Aase, Equinor; Geir Olav Ånesbug, Jagtech

This paper has been accepted for presentation at the Abu Dhabi International Petroleum Exhibition & Conference, 15-18 November 2021

Abstract:

Objectives/Scope: In this work, a measurement system is described that can be easily deployed in the rig site to find the mass of magnetic contaminations in the drilling fluid samples since there is a lack of established standard procedures in the oil and gas industry to serve this purpose. Use of this method helps us figure out when more e!ort needs to be made to treat the drilling fluid and improve the ditch magnet system's effciency. These magnets are usually placed in the flowline, upstream shale shakers on a drilling rig to clean magnetic contaminations.
Methods, Procedures, Process: A magnet rod, same as those used in the ditch magnet system, was utilized to measure the mass of the magnetic contamination. An extensive set of drilling fluid samples were tested. The samples were collected from a North Sea drilling operation. A scanning electron microscope (SEM) test was performed on the collected magnetic sample to analyze and determine the source of the magnetic contaminations.

Results, Observations, Conclusions: This method showed good effciency in collecting the magnetic particles and hence measuring the weight of them. Results from using an e"cient ditch magnet system at the Ivar Aasen field in the North Sea show that a sufcient amount of magnetic debris can be removed to increase the accuracy of the downhole directional measurements. The ditch magnets used in the drilling operation where the current samples were collected were not optimized in performance to the same degree as being the case at the Ivar Aasen field. Current results show that the drilling fluids obtained downstream of these mounted ditch magnets still contained small-sized worn metal particles caused by the casing and downhole equipment abrasion. The content of magnetic debris after the ditch magnets at the Ivar Aasen field is anticipated to be less.

Novel/Additive Information: One of the major sources of magnetic interference is the drilling fluid, which shields the measurement of the cross-axial components of the earth's magnetic field measured by magnetometers. Despite this important fact, there is no standard method to measure the magnetic content of drilling fluid. This work aims to establish a measuring system that satisfies this objective.